State space analysis of power distribution networks for studying voltage sensitivity

Kestutis Samulis

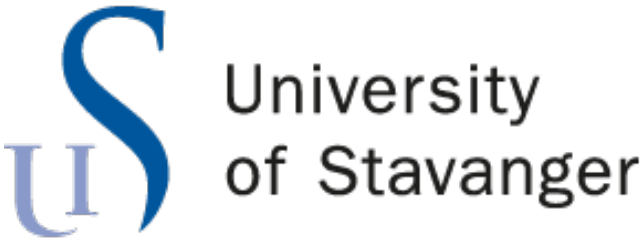

Master's program in robotics technology and signal processing

at

University of Stavanger

Department of Electrical Engineering and Computer Science

June 1, 2024

Acknowledgements

I want to thank my supervisor Merkebu Zenebe Degefa and my co-supervisor Damiano Rotondo for their outstanding guidance, encouragement, thoughtful comments, and valuable feedback. I would also like to thank my family and friends for their support and motivation.

Abstract

Power generation is transitioning away from centralized electricity generation facilities with the increase of energy consumption from renewable sources, such as solar and wind. Along with rising demand for electric vehicle charging, this shift strains the electric grid. With limited energy storage options, most generated energy must be consumed immediately. To deliver energy efficiently, voltage and frequency must be maintained at stable levels. The integration of distributed renewable sources, directly connected to the distribution grid, can produce large variations in supply and demand, reducing efficiency. This increases the complexity of operations and requires improved methods for network monitoring and control. In this thesis, a modified case4_dist distribution network is used to develop a dynamic model in state-space form to analyze voltage sensitivity and transient response in the system. The performance of the dynamic model is compared with solutions of power flow equations solved using the well-established Newton-Raphson method. The results show that the discrepancy between the models is minimal. The voltage sensitivity analysis reveals how load changes affect the bus voltages of the network. Transient voltage response analysis shows high voltage variation and the rapid convergence to the nominal values. The model can be integrated with advanced analysis and control design to improve the efficiency and reliability of distribution network operations, and it is proposed as future work.

Abbreviations

AC	Alternating Current
B	Susceptance
DC	Direct Current
G	Conductance
J	Jacobian
KCL	Kirchhoff's Current Law
KVL	Kirchhoff's Voltage Law
LTI	Linear Time-Invariant
MIM0	Multiple Input, Multiple Output
NR	Newton-Raphson
P	Active Power
pu	Per Unit
Q	Reactive Power
R	Resistance
RMS	Root Mean Square
S	Apparent Power
SIMO	Single Input, Multiple Output
SVD	Singular Value Decomposition
X	Reactance
Z	Impedance
Y	Admittance

Contents

List of Figures

Chapter 1

Introduction

1.1 Motivation

The European Environmental Agency (EEA) provides an analysis on the share of energy consumption from renewable sources in Europe. EEA states that, according to Eurostat the renewable energy share in Europe is 23 % [7] and is expected to continue growing [1].

This increase in renewable energy sources indicates a shift from centralized energy production facilities to distributed generation of energy from renewable sources [16]. This bring issues in effectively controlling the voltage stability in the distribution network. Since there are limitations in storing produced energy, most of it must be consumed immediately. The renewable energy sources that are directly connected to the distribution grid can produce large variations that can affect voltage stability of the power grid.

Voltage sensitivity provides insight into how different load conditions affect voltage levels in the distribution network and helps to ensure voltage stability [8]. The motivation behind this thesis is to construct a reduced yet sufficiently accurate dynamic model of a power distribution network to efficiently compute the sensitivity of voltage magnitude and angle with respect to changes in active and reactive power demand.

1.2 Problem Statement

To analyze voltage sensitivity, gramian matrix can be obtained trough conventional methods, such as Newton-Raphson method, that show how changes in active and reactive power injections at different buses of the distribution network affects the relative voltages. These conventional algorithms can be computationally demanding to calculate for large systems.

The goal is to develope a dynamic model of the system that is that is sufficiently accurate to perform voltage stability analysis.

1.3 Thesis Outline

1. Background and Models
2. Two-Bus System Model Defined by Power Flow Equations.
3. Dynamic Model in State-Space Form of a Two-Bus System.
4. Dynamic Model in State-Space Form of a Four-Bus System.
5. Discussion of Reduction Methods
6. Two-Bus Model Performance Comparison.
7. Voltage Sensitivity Analysis of the Four-Bus Network.
8. Transient Response Analysis.
9. Conclusion

Chapter 2

Background

In this chapter, a short introduction to the power grid is provided. The study case of the case4_dist model is presented and discussed. The conversion between the three-phase and single-phase equivalent circuits is explained, along the relevant equations for this thesis. A concise derivation of the power flow equations is demonstrated. The Newton-Raphson algorithm and state-space representation of a system is introduced. The π equivalent representation of the transmission lines is discussed. The voltage sensitivity analysis is described. Finally, various methods used for dynamic model reduction are mentioned, with a focus on the Singular Value Decomposition method.

2.1 Introduction to Power Grid Networks

A power grid is a sophisticated network comprised of generators, transformers, and substations which are interconnected by distribution lines that transmit the electric power to the consumers. Electricity must be delivered reliably and efficiently across multiple voltage levels in order to meet the varying demand.

Figure 2.1 is a one-line diagram of a power grid system that shows the different parts the grid can be subdivided into. The transmission grid transports the electricity over long distances at high-voltage (400-300kV) from the generation sources to the distribution networks. The operation at high voltage allows to reduce energy losses and efficiency improvement over long distances. [6].

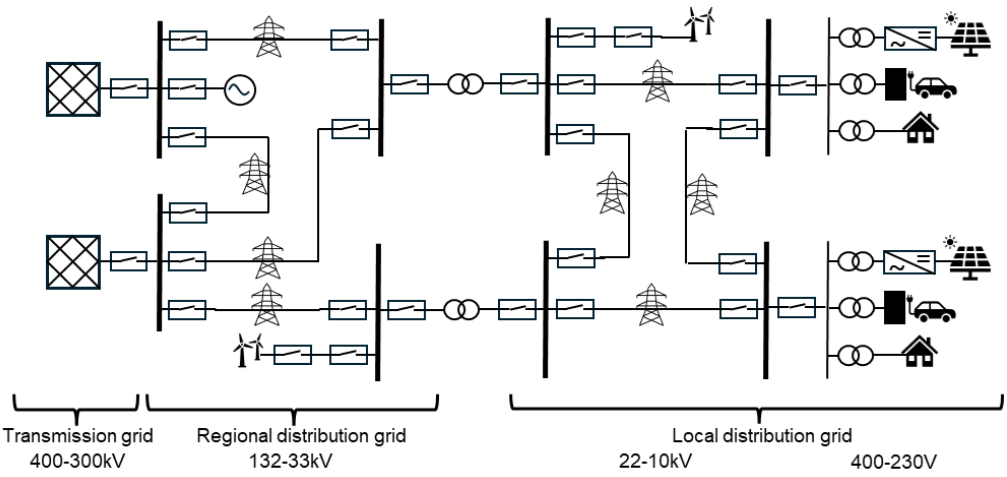

Figure 2.1: One-line diagram of the power grid network

The regional distribution grid is a medium voltage network (132-33kV) that transmits electricity form the transmission grid to various local distribution networks and power intensive industrial consumers. The voltage levels are managed and distributed form the substations to ensure stable and reliable power delivery. The local distribution grid, operating at 22-10 kV for industrial users and 400-230 V for residential and small commercial users, represents the final step in electricity

distribution, where voltage is stepped down to levels suitable for end-users [6].

The increasing load demand and the integration of decentralized energy generation sources, such as wind and solar, in distribution grids is presenting challenges regarding voltage stability [12]. Significant deviations in voltage levels from their nominal values at the substations can lead to reduced efficiency of power delivery, equipment malfunctions or power outages. Therefore, it is important to monitor the impact that load changes have on different nodes within the power grid and to take the appropriate actions to mitigate the voltage discrepancies.

2.2 The case4_dist Distribution Network Model

The models studied in this thesis are based on a modified version of a case4_dist system found in the MATPOWER simulation software. This system originally comprises 4 buses and 2 generators. The modification lies in the second bus, where a generator is substituted by a load (PQ), as presented in Figure 2.2

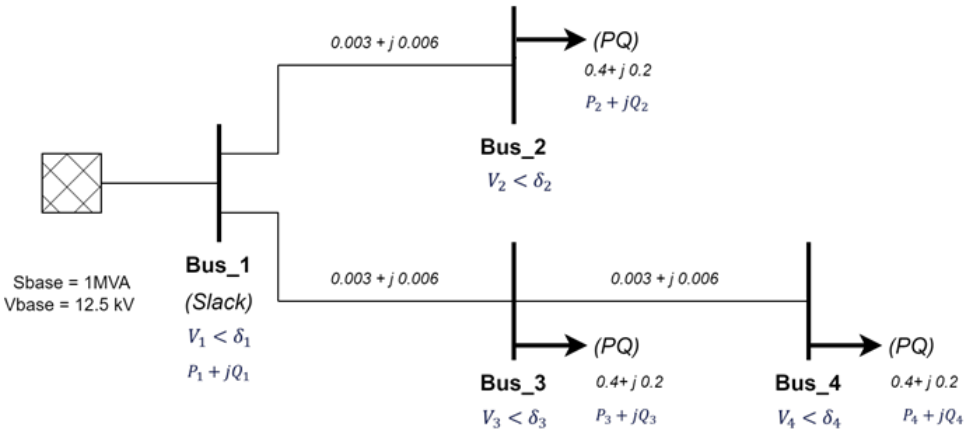

Figure 2.2: Modified case4 dist system

This model represents the high voltage local distribution grid, with a voltage range of 22kV to 10kV. The load and impedance units in the diagram are presented in the per unit (pu) system, which in this case, normalizes the system quantities to a common base of 1MVA of apparent power (S_b) and 12.5kV for base voltage (V_b). Each bus is connected by transmission lines with equal impedance, having a resistance of 0.003 pu and a reactance of 0.006 pu. Buses 2, 3 and 4 have loads connected to them that consume 0.4 pu of active power and 0.2 pu of reactive power. First bus (slack bus) injects power into the system to keep it balanced and acts as a reference point. The chosen frequency at which the system operates is $f = 50$Hz. The angular frequency is then $\omega = 2\pi f = 100\pi$.

A bus is a set of three nodes corresponding to the three phases of the power system where different components, such as generators, loads, transformers, and transmission lines, are connected. A system that is balanced, time-invariant, and with normalized values can be analyzed as an equivalent single-phase system with only one node representing a bus, as presented in Figure 2.2 [14]. Each bus is associated with four quantities:

- V_i: voltage magnitude at i^{th} bus
- δ_i: phase angle at i^{th} bus
- P_i: injected active power at i^{th} bus
- Q_i: injected reactive power at i^{th} bus

Depending on which of the above quantities are known the buses can be categorized as a slack bus, generator bus or a load bus as indicated in the Table 2.2.

Table 2.1: Bus types and variables

Bus Type	**Known quantities**	**Unknown quantities**
Slack bus (Ref.)	$\|V\|, \delta$	P, Q
Generator bus (PV)	P,$\|V\|$	Q, δ
Load bus (PQ)	P, Q	$\|V\|, \delta$

- **Slack bus**, also known as swing bus, is a reference point for voltage magnitude, set typically at 1 p.u., and phase angle set at 0 degrees, that accounts for variations in transmission lines to maintain a power balance in the system. The active and reactive power are unknown variables but can be determined trough calculations.

- **Generator buses**, also known as PV buses, denotes nodes where power is injected into the system by energy sources, such as power plants. The reactive power and the voltage magnitude are known values.

- **Load buses**, also known as PQ buses, since the real and reactive power of the bus are known values. It represent the nodes where power is consumed, such as residential buildings or industrial facilities.

A N-bus system can be depicted as the sum of all its constituent bus types expressed by the Equation 2.1. The n_{PV} term represents the number of generator buses, n_{PQ} indicates the number of load buses, and the addition of 1 accounts for the slack bus in the system.

$$N = n_{PV} + n_{PQ} + 1 \tag{2.1}$$

Table 2.2: Power Flow Equations by Bus Type

Bus Type	**Number of Power Flow Equations per Bus Type**
Slack	0
PV	n_{PV}
PQ	$2(N - n_{PV} - 1)$

2.3 Three-Phase Network and the Single-Phase Equivalent

In order to correctly convert the distribution network values, such as impedance and apparent power, from a three-phase system to an equivalent single-phase circuit, the system needs to be balanced and the type of connection between the windings of a generator or a transformer and the load must be known. There are two types of connections: Y-connection and Δ-connection, as shown in Figure 2.3

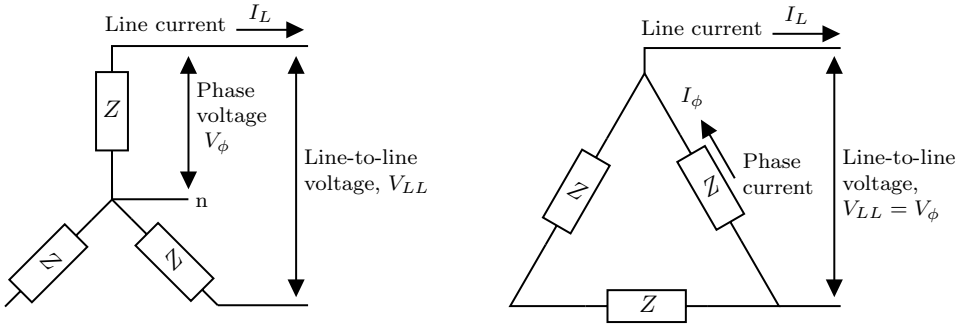

a) Y-connection b) Δ-connection

Figure 2.3: Y- and Δ-connection diagrams

For the Y-connection, each phase is connected to a common neutral point. Assuming a balanced system, the current flowing in each phase is equal in magnitude. The sum of the currents flowing trough the neutral point is zero and therefore, the current in the neutral line is also zero. The phase voltage is measured between the phase and the neutral point, while the line-to-line voltage is measured between phases. The phase voltage is lower than a line-to-line voltage by a factor of $\sqrt{3}$, as presented in Equation 2.2

$$|V_{LL}| = \sqrt{3}|V_\phi| \tag{2.2}$$

For the Δ-connection, each phase is connected end-to-end in a closed loop. The phase voltage and line-to-line voltage are equal in magnitude since there is only the line-to-line voltage. In contrast to the Y-connection, the Δ-connection phase current is proportional to the line current by a factor of $\sqrt{3}$, as shown in Equation 2.3

$$|I_L| = \sqrt{3}|I_\phi| \tag{2.3}$$

When converting a three-phase system to a single-phase circuit, this has to be taken into consideration. In actual distribution networks, this information would be provided by the utility company. However, for the purposes of this thesis, it is assumed that all connections between transformer and load windings are Y-connected. This assumption is made because voltage sensitivity is the primary focus, and Y-connections simplify the analysis.

In Figure 2.2 of the modified case4_dist model, the load apparent power is presented as the total average power that the load consumes. For a single-phase circuit, this power consumption has to be scaled by a third, since it is the power consumed per phase, as indicated in Equation 2.4. This is equivalent to scaling the line-to-line voltage and line current by a factor of $\sqrt{3}$.

$$S_{3\phi} = 3S_{1\phi} = \sqrt{3}|V_{LL}||I_L| \tag{2.4}$$

To find the actual values for transmission line impedance from the per unit values provided in the case4_dist diagram, the base apparent power, S_b, and the base voltage, V_b, must first be converted to single-phase values, using Equations 2.2 and 2.4. The line base impedance, Z_b can then be calculated using the relation shown in Equation 2.5. Afterwards, the transmission line impedance can be directly scaled by the line base impedance Z_b.

$$\left|S_{1\phi}\right| = \left|V_\phi\right|\left|I_\phi\right| = \frac{\left|V_\phi\right|^2}{Z_b} \tag{2.5}$$

The effective voltage value of an AC voltage waveform is the root mean square voltage, V_{rms}, which is equivalent to the DC voltage that would deliver the same power. The voltage base value, V_b of 12.5kV, specified in case4_dist diagram, is the RMS voltage. When used as an input sinusoidal signal in a single-phase circuit, the RMS voltage, V_{rms}, must be converted to the peak voltage value V_{peak}, as indicated by Equations 2.6, so that the oscillating input signal V_s is scaled correctly, as shown in Equation 2.7.

$$V_{rms} = \frac{V_{peak}}{\sqrt{2}} \tag{2.6}$$

$$V_s = V_{peak} \sin(\omega t + \theta) \tag{2.7}$$

2.4 Power Flow Equations

The flow of power in a power grid is described by complex nonlinear equations, which forms the basis for calculating the phase angle and magnitude of the voltage at each bus, along with determining the flow of active and reactive power through the transmission lines [13]. A brief derivation is presented below.

According to Kirchhoff's current law, the injected current is defined as the sum of currents flowing into the bus, which can be expressed as the sum of the products between each bus voltage, V_k and the admittance Y_{ik} between the respective buses, denoted in Equation 2.8, where N signifies the total number of buses within the system.

$$I_i = \sum_{k=1}^{N} Y_{ik} V_k \tag{2.8}$$

The power vector in the complex plane is equal to the product of bus voltage and the complex conjugate of the current. This can also be expressed as the sum of active and reactive power, as shown in Equation 2.9.

$$S_i = V_i I_i^* = V_i (\sum_{k=1}^{N} Y_{ik}^* V_k^*) = P_i + jQ_i \tag{2.9}$$

The phase angle, δ_i, is the angle between the voltage vector V_i at bus i and the reference axis. The same applies to the voltage vector at a bus k, but the phase angle δ_k is negative due to its complex conjugate.

$$V_i = |V_i| \, e^{j\delta_i} \tag{2.10}$$

$$V_k^* = |V_k| \, e^{-j\delta_k} \tag{2.11}$$

Line admittance Y is the reciprocal of the line impedance Z. The admittance can be expressed as the sum of conductance G and susceptance B, which are the inverse of resistance R and reactance X, respectively. In this case, the conjugate of the admittance results in a negative angle when represented in exponential form.

$$Y_{ik}^* = G_{ik} - jB_{ik} = |Y_{ik}| \, e^{-j\theta_{ik}} \tag{2.12}$$

Substituting Equations 2.10, 2.11 and 2.12 into Equation 2.9, results in the complex power, where the sum of the bus voltages of the system and the transmission line admittance between the respective buses with the corresponding angles is equal to the sum of active power P_i and reactive power Q_i, as presented in Equations 2.13.

$$S_i = \sum_{k=1}^{N} |V_i||V_k||Y_{ik}| \, e^{j(\delta_i - \delta_k - \theta_{ik})} = P_i + jQ_i \tag{2.13}$$

The complex power can be divided into two equations; P_i, containing all the components in the real plane, Equation 2.14, and Q_i, encompassing the components in the imaginary plane, Equation 2.15. The change in angle sign, as well as of the reactive power, is due to the even and odd symmetry of cosine and sine functions, respectively.

$$P_i = \sum_{k=1}^{N} |V_i||V_k||Y_{ik}| \cos(\delta_k - \delta_i + \theta_{ik}) \tag{2.14}$$

$$Q_i = -\sum_{k=1}^{N} |V_i||V_k||Y_{ik}| \sin(\delta_k - \delta_i + \theta_{ik}) \tag{2.15}$$

The resulting Equations 2.14 and 2.15 are called power flow equations. The solutions to these equations allow to determine the flow of power under steady-state conditions. However, due to the nonlinear nature of these functions, which involve squared voltage terms and trigonometric functions, finding the solutions requires the use of iterative methods.

2.5 Newton-Raphson Algorithm

Solving the power flow equations for a bus voltage magnitude, $|V|$, and phase angle, δ, involves the use of a numerical method, since the equations are nonlinear. There are a few numerical methods that can be used to find the solutions, such as Gauss-Seidel and Newton-Raphson (NR) iterative method. Newton-Raphson is a well known method that is widely used in the power network analysis because of its robust and simple implementation.

With the NR method, the unknown voltage magnitudes and phase angles can be approximated by finding the roots of the power flow functions, using an iterative process. Essentially, the objective is to minimize the difference between the specified injected power, $P^{(specified)}$, which represents the difference between the generated and demanded power, and the calculated power $P^{(calculated)}$, aiming to converge it to zero. This is called the mismatch power and is presented in Equations 2.16.

$$\begin{aligned} \Delta P_i &= P_i^{(\text{specified})} - P_i^{(\text{calculated})} \\ \Delta Q_i &= Q_i^{(\text{specified})} - Q_i^{(\text{calculated})} \end{aligned} \tag{2.16}$$

To achieve this objective, it is necessary to linearize the the system around the current operating point. Equations presented in 2.14 and 2.15. The linear approximation can achieved via first-order Taylor series expansion around some initial values δ_0 and V_0 as demonstrated in Equations 2.17, where $\Delta\delta_k$ and ΔV_k represent the correction values for angle and voltage magnitude, respectively.

$$\begin{aligned} P_i &\approx P_i(\delta_k^0 ... \delta_N^0, V_k^0 ... V_N^0) + \sum_{k=2}^{N} \frac{\partial P_i}{\partial \delta_k} \Delta\delta_k + \sum_{k=2}^{N} \frac{\partial P_i}{\partial V_k} \Delta V_k \\ Q_i &\approx Q_i(\delta_k^0 ... \delta_N^0, V_k^0 ... V_N^0) + \sum_{k=2}^{N} \frac{\partial Q_i}{\partial \delta_k} \Delta\delta_k + \sum_{k=2}^{N} \frac{\partial Q_i}{\partial V_k} \Delta V_k \end{aligned} \tag{2.17}$$

The mismatch power equations presented in 2.16 are derived by relocating the first terms from the right side of Equations 2.17 to the left side. Performing this procedure for every bus in the system where the voltage magnitudes and angles need to be determined will yield in a system of linear equations that can be represented in matrix form, as follows:

$$\begin{bmatrix} \boldsymbol{\Delta P} \\ \boldsymbol{\Delta Q} \end{bmatrix} = \begin{bmatrix} \boldsymbol{J}_{P\delta} & \boldsymbol{J}_{PV} \\ \boldsymbol{J}_{Q\delta} & \boldsymbol{J}_{QV} \end{bmatrix} \begin{bmatrix} \boldsymbol{\Delta\delta} \\ \boldsymbol{\Delta|V|} \end{bmatrix} \tag{2.18}$$

In Equation 2.18, the mismatch vector $[\boldsymbol{\Delta P}, \boldsymbol{\Delta Q}]^T_{N\times 1}$, which contains active and reactive power mismatch values, is computed as the product of the Jacobian matrix, $[\boldsymbol{J}]_{N\times N}$ and the correction vector $[\boldsymbol{\Delta\delta}, \boldsymbol{\Delta|V|}]^T_{N\times 1}$, formed by the phase angle and voltage magnitude correction values.

The Jacobian is composed of four sub-matrices, as shown in 2.19. The elements of $\boldsymbol{J}_{P\delta}$ and $\boldsymbol{J}_{Q\delta}$ contain the the partial derivatives of active and reactive power with respect to phase angle, respectively. The matrix dimension of $\boldsymbol{J}_{P\delta}$ is $(n_{PV}+n_{PQ})\times(n_{PV}+n_{PQ})$, while the size of $\boldsymbol{J}_{Q\delta}$ is $(n_{PV}+n_{PQ})\times n_{PQ}$. Similarly, $\boldsymbol{J}_{PV}$ and $\boldsymbol{J}_{QV}$ are partial derivative matrices of active and reactive power with respect to the voltage magnitude. $\boldsymbol{J}_{PV}$ has size $n_{PQ}\times(n_{PV}+n_{PQ})$, while $\boldsymbol{J}_{QV}$ is of dimension $n_{PQ}\times n_{PQ}$.

$$\boldsymbol{J} = \left[\begin{array}{cc} \boldsymbol{J}_{P\delta} & \boldsymbol{J}_{PV} \\ \boldsymbol{J}_{Q\delta} & \boldsymbol{J}_{QV} \end{array}\right] = \left[\begin{array}{ccccc} \frac{\partial P_2}{\partial \delta_2} & \cdots & \frac{\partial P_2}{\partial \delta_N} & \frac{\partial P_2}{\partial |V_2|} & \cdots & \frac{\partial P_2}{\partial |V_N|} \\ \vdots & \ddots & \vdots & \vdots & \ddots & \vdots \\ \frac{\partial P_i}{\partial \delta_2} & \cdots & \frac{\partial P_i}{\partial \delta_N} & \frac{\partial P_i}{\partial |V_2|} & \cdots & \frac{\partial P_i}{\partial |V_N|} \\ \hline \frac{\partial Q_2}{\partial \delta_2} & \cdots & \frac{\partial Q_2}{\partial \delta_N} & \frac{\partial Q_2}{\partial |V_2|} & \cdots & \frac{\partial Q_2}{\partial |V_N|} \\ \vdots & \ddots & \vdots & \vdots & \ddots & \vdots \\ \frac{\partial Q_i}{\partial \delta_2} & \cdots & \frac{\partial Q_i}{\partial \delta_N} & \frac{\partial Q_i}{\partial |V_2|} & \cdots & \frac{\partial Q_i}{\partial |V_N|} \end{array}\right] \tag{2.19}$$

The indexing start at $k = 2$, since it is assumed that the first bus is the slack bus for which the voltage magnitude and the phase angles are known.

To find the values of interest, that are phase angle and voltage magnitude, the inverse of the Jacobian matrix has to be performed as shown in Equation 2.20. The Jacobian matrix must be invertible, for the solution to converge.

$$\begin{bmatrix} \Delta\delta_2 \\ \vdots \\ \Delta\delta_N \\ \Delta|V_2| \\ \vdots \\ \Delta|V_N| \end{bmatrix} = \begin{bmatrix} \boldsymbol{J}_{P\delta} & \boldsymbol{J}_{PV} \\ \boldsymbol{J}_{Q\delta} & \boldsymbol{J}_{QV} \end{bmatrix}^{-1} \begin{bmatrix} \Delta P_2 \\ \vdots \\ \Delta P_N \\ \Delta Q_2 \\ \vdots \\ \Delta Q_N \end{bmatrix} \tag{2.20}$$

Finally, phase angle and voltage magnitude are approximated by the NR method presented in Equation 2.21 for which an iterative process is required.

$$\boldsymbol{X_{n+1}} = \boldsymbol{X_n} - [\boldsymbol{J}(\boldsymbol{X_n})]^{-1}\boldsymbol{F}(\boldsymbol{X_n}) \tag{2.21}$$

In each iteration the tolerance is checked, which is the difference between the current and the previous solutions. If the tolerance is met, the solution has converged. This process is illustrated in Figure 2.4 as a flow chart.

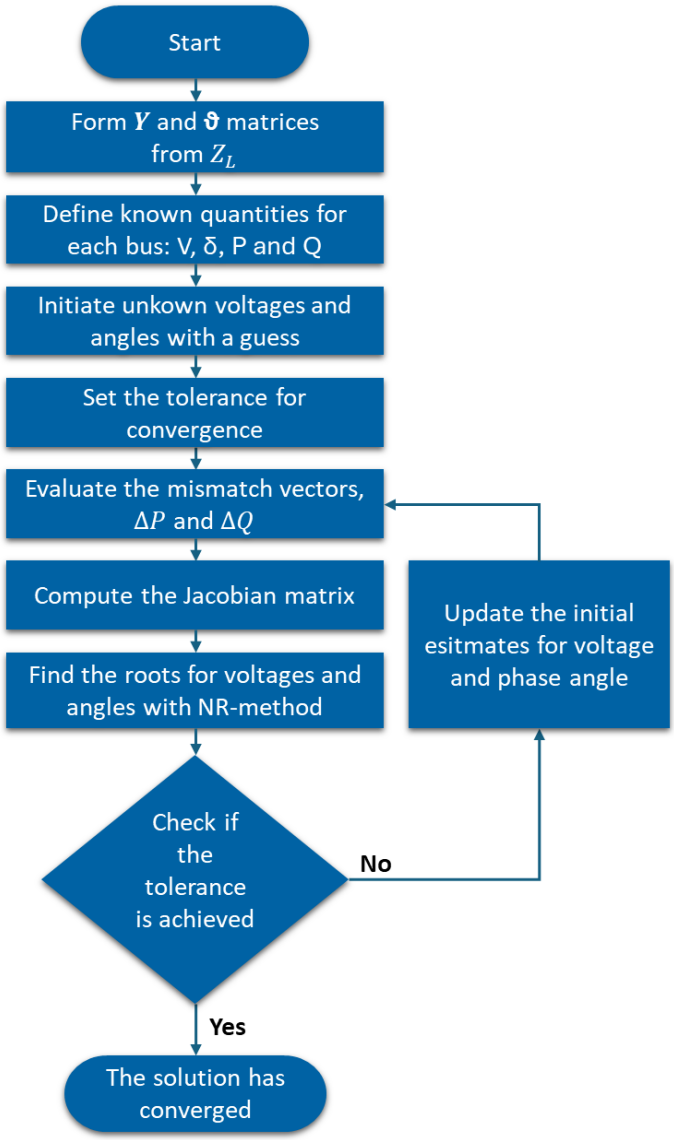

Figure 2.4: Newthon-Raphson algorithm flow chart

The convergence speed of the Newton-Raphson method depends largely on the number of iterations that the algorithm has to perform to converge to a solution. Convergence is not always guaranteed. If the Jacobian matrix is becomes singular, the solution will diverge. Therefore, it is good practice to make the initial guess as close to the actual solution as possible.

2.6 State-Space Model

State space of a system is an n-dimensional space in which each axis corresponds to one of the state variables of the system. State variables are the minimal set of variables that uniquely determine the state of the system at any given time [9]. The number of state variables in the distribution grid network can be defined by the number of components that store energy in the system. The modified case4_dist model can be converted into, a continuous, time-invariant (LTI), single-input, multiple-output (SIMO) system. Although, multiple-input, multiple-output (MIMO) is more realistic for real-life applications since there is more than one voltage source connected to the distribution grid, the focus is on the study of the modified case4_dist model behaviour.

State space model can be expressed using the state equations, that are n simultaneous first-order differential, linearly independent equations that describe the dynamics of the system, Equation

2.22, and the output equation that describes the relationship between the states and the output, Equation 2.23 [9]:

$$\dot{\boldsymbol{x}}(t) = \boldsymbol{f}(t, \boldsymbol{x}(t), \boldsymbol{u}(t)) \tag{2.22}$$

$$\boldsymbol{y}(t) = \boldsymbol{g}(t, \boldsymbol{x}(t), \boldsymbol{u}(t)) \tag{2.23}$$

$$\boldsymbol{x}(t_0) = \boldsymbol{x}_0 \tag{2.24}$$

Where:

- $\dot{\boldsymbol{x}}(t)$ is the derivative of the state vector with respect to time
- $\boldsymbol{x}(t)$ is the state vector
- $\boldsymbol{u}(t)$ it the input vector
- $\boldsymbol{y}(t)$ is the output vector
- $\boldsymbol{x}_0$ is the initial state

If the state equations are nonlinear, they must be linearized around the operating point before they can be expressed in matrix form as follow:

$$\begin{aligned} \dot{\boldsymbol{x}}(t) &= \boldsymbol{A}\boldsymbol{x}(t) + \boldsymbol{B}\boldsymbol{u}(t) \\ \boldsymbol{y}(t) &= \boldsymbol{C}\boldsymbol{x}(t) + \boldsymbol{D}\boldsymbol{u}(t) \end{aligned} \tag{2.25}$$

- $\boldsymbol{A} \in \mathbb{R}^{n \times n}$ is the state matrix
- $\boldsymbol{B} \in \mathbb{R}^{n \times m}$ is the input matrix
- $\boldsymbol{C} \in \mathbb{R}^{p \times n}$ is the output matrix
- $\boldsymbol{D} \in \mathbb{R}^{p \times m}$ is the direct transmission matrix

There are multiple state-space representations for the same system, meaning that the representation for a given system is not unique. This is because there are various ways to arrange state-space equations to form the state matrix. However, these different representations do not alter the underlying system [9].

With the system expressed in state-space, various control techniques can be applied, such as state feedback control, observer-based control, optimal control (LQR) alongside the tools to analyze observability and controllability of a system. It also provides the possibility for state estimation, fault detection, and real-time monitoring.

In electric circuits, the state variables are typically chosen as the voltage across capacitors and the currents through the inductors since these are the components that have an influence on the behaviour the system over time.

2.7 The π-Model Representation of a Transmission Line

For the modified case4_dist model, a π-model equivalent circuit can be used to represent the transmission lines. The π-model is a sufficiently accurate for modeling medium-voltage transmission lines, as is in case4_dist network, provided that the line length per π-model does not exceed 150km. However, for fast transient responses over very short periods, the π-model may not provide accurate results and a wave equation should be used instead [3]. In Figure 2.5 a representation of a π-model as one-line diagram is shown.

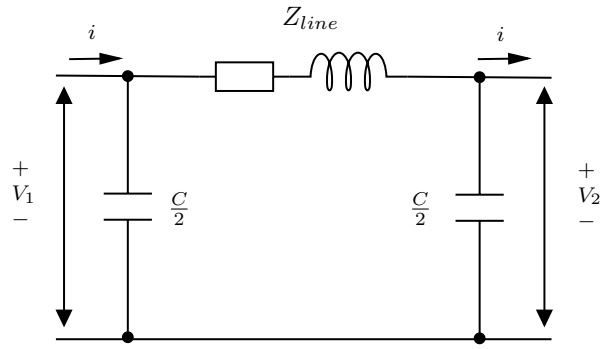

Figure 2.5: π-model for a medium voltage transmission line

The π-model captures the characteristics of a transmission line, including its resistance, inductance, and capacitance. The capacitors represent the shunt capacitance between the transmission line and the ground. For long transmission lines, the effects of shunt capacitances and the line impedance needs to be considered as continuously distributed quantities along the lenght of the line.

2.8 Voltage Sensitivity Analysis

To meet the load demand and maintain normal operating conditions in the power grid system, voltage levels must be maintained within specified operating limits at all buses in the network. Thus, voltage stability is crucial for grid stability, equipment protection and efficient power transmission and distribution [2].

Sensitivity analysis is a relatively simple but powerful method that allows to study how the variations in systems inputs impact the system behaviour in a manner that is easy to conceptualize. This analytical approach provides insights into the magnitude of the impact that each input has on the overall behaviour of the system [17]. The sensitivity coefficients are determined when the solution reach convergence and effect of the small changes of voltage magnitude and phase angle that have on the system can be interpreted [10]. For a multi-variable system, the sensitivities can be expressed in a Jacobian matrix as presented in 2.26.

$$\begin{bmatrix} \frac{\partial f_1}{\partial x_1} & \cdots & \frac{\partial f_1}{\partial x_n} \\ \vdots & \ddots & \vdots \\ \frac{\partial f_m}{\partial x_1} & \cdots & \frac{\partial f_m}{\partial x_n} \end{bmatrix} \tag{2.26}$$

Power distribution networks, which typically are comprised of complex, large-scale systems, are commonly approximated with high-dimensional, nonlinear models. These factors make it computationally costly to analyse and predict the system behaviour [18]. With the state-space model of the network, the sensitivity analysis can be directly performed by monitoring how load changes affect the voltage levels at different buses in the system.

2.9 Dynamic Model Reduction

In article [5], Savo D.Dukić and Andrija T.Sarić have proposed several reduction techniques for linear dynamic systems. The proposed techniques are following:

- Singular Perturbation Analysis (SPA)
- Modal Analysis (MA)
- Singular Value Decomposition (SVD)
- Moment Matching (MM)

- SVD-Krylov Methods, which is a combination of SVD and MM

From the proposed techniques, singular was attempted to implement in this thesis. The singular value decomposition is a technique used to mitigate large amounts of data in matrices by expressing the matrix as follow [11]:

$$A = U\Sigma V^T \tag{2.27}$$

Where:

- U is an $m \times m$ size orthogonal matrix
- Σ is and $m \times n$ diagonal matrix composed of singular values
- V is an $n \times n$ orthogonal matrix

This technique allows to interpret the structure of matrices with large dateset, which in power distribution can occur for large networks. The vectors in U matrix and the singular values in Σ are ordered in decreasing order of magnitude. The ordering helps identifying the most significant components of the matrix, making it useful for dimensionality reduction by truncating the less influential data set [5].

The application of this technique was attempted on the state matrix of the two-bus and the four-bus dynamic model. However, the state matrices are not sufficiently large, resulting in no significant differences between singular values. A naive attempt was made truncating the $U\Sigma V^T$ matrices, but this altered the systems behaviour and made this approach ineffective in these particular cases.

Chapter 3

Analysis case and methods

This chapter introduces the models and the methods used to perform voltage sensitivity and transient response analysis. For each model and method, the underlying equations, the choice of values, and the calculations are explained. First, the two-bus system is introduced, for which the Newton-Raphson method is used, and from which the dynamic model in state-space is derived. Following this, the two bus system created in MATLAB Simscape is introduced and discussed. Finally, the dynamic model of the full four-bus system is presented.

3.1 Newton-Raphson Method Applied to the Two-Bus System

The goal with the iterative approach of Newton-Raphson method is to find the voltage magnitude and the phase angle at the second bus employing the power flow equations, discussed in Section 2.5. A simplified version of the modified case4_dist model with only two buses is presented in Figure 3.1.

The generator is connected to the load via a transmission line with an impedance of $Z_{line} = 0.003 + j0.006$ pu. S_1 and S_2 represent the apparent power that is supplied and consumed by the generator and the load, respectively. The apparent power for the load is given as $P_2 = 0.4$ pu and $Q_2 = 0.2$ pu in the modified case4_dist model. The apparent power for the generator is not specified, but it is not strictly necessary to know since there is enough information to find the solutions. The bus connected to the generator also functions as a slack bus since there is only one generator in the system. The values of voltage magnitude, V_1 and phase angle, δ_1 are known to be 1 pu and 0 degrees, respectively. For the second bus, voltage magnitude, V_2 and phase angle, δ_2 are unknown and need to be determined using the Newton-Raphson method.

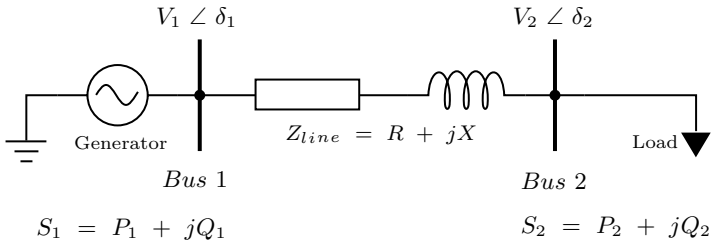

Figure 3.1: Single-line diagram of two-bus system

For every bus in the system, there are two equations that describe the power flow. In this case of a two-bus system, only two equations are necessary since only the voltage magnitude and the phase angle for the second bus need to be calculated. The mismatch equation for the active power, denoted as f_{P_2} is shown in Equation 3.1, and for the reactive power, denoted as f_{Q_2} is presented in Equation 3.2. Active power, P_2, and reactive power, Q_2 are the specified load values. The mismatch equations are referred to in Equation 2.16, and discussed in Section 2.5.

$$f_{P_2} = |V_1 V_2 Y_{21}|\, cos(\delta_1 - \delta_2 + \theta_{21}) + \left|V_2^2 Y_{22}\right| cos(\theta_{22}) - P_2 \tag{3.1}$$

$$f_{Q_2} = -|V_1 V_2 Y_{21}|\, sin(\delta_1 - \delta_2 + \theta_{21}) - \left|V_2^2 Y_{22}\right| sin(\theta_{22}) - Q_2 \tag{3.2}$$

The admittance matrix, also known as Y-bus matrix, shows the relation between the bus voltages and the injected currents in the transmission line. Using the admittance instead of the impedance simplifies the process of solving the power flow equations. To calculate the admittance matrix the Kirchhoff's current law (KCL) is applied to the line, as shown in Figure 3.2, where currents i_1 and i_2 are the currents entering and leaving the transmission line seen from each bus's perspective. In this case, this can be expressed in two equations an put in matrix form, as shown in Equation 3.3.

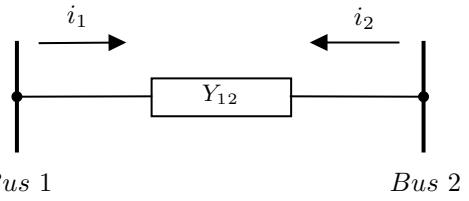

Figure 3.2: Current flow through the transmission line.

$$\begin{bmatrix} I_1 \\ I_2 \end{bmatrix} = \begin{bmatrix} Y_{11} & -Y_{12} \\ -Y_{21} & Y_{22} \end{bmatrix} \begin{bmatrix} V_1 \\ V_2 \end{bmatrix} \tag{3.3}$$

Since the line admittance is a complex number and the power flow equations are split into two real-valued equations that require the admittance magnitude and the angle, the Y-matrix is decomposed into two matrices: one containing the admittance magnitudes and the other containing the respective angles, as presented in Equations 3.4 and 3.5, respectively.

$$|\boldsymbol{Y}| = \begin{bmatrix} Y_{11} & Y_{12} \\ Y_{21} & Y_{22} \end{bmatrix} \tag{3.4}$$

$$\boldsymbol{\theta} = \begin{bmatrix} \theta_{11} & -\theta_{12} \\ -\theta_{21} & \theta_{22} \end{bmatrix} \tag{3.5}$$

The mismatch Equations 3.1 and 3.2 are nonlinear due to trigonometric and exponential functions. Therefore, they must be linearized around an operating point. Since the operating point is unknown, reasonable a guess of the solution must be made to achieve convergence. In this case, the initial values chosen are $V_2^0 = 1$ pu, for the voltage magnitude and $\delta_2^0 = 0°$, for the phase angle.

The four linearized equations for the two-bus system form the Jacobian matrix, as shown in Equation 3.6. These elements indicate how sensitive the power mismatch equations are to changes in voltage magnitude and phase angle at the second bus, as discussed in Section 2.5.

$$\boldsymbol{J} = \begin{bmatrix} J_{11} & J_{12} \\ J_{21} & J_{22} \end{bmatrix} \tag{3.6}$$

Elements J_{11} and J_{21} are the partial derivatives of the active power mismatch equation with respect to the phase angle and the voltage magnitude, respectively, as presented in Equations 3.7 and 3.9. Similarly, elements J_{12} and J_{22} are the partial derivatives of the reactive power mismatch equation with respect to the same variables as indicated in Equations 3.8 and 3.10.

$$J_{11} = \frac{\partial f_{P_2}}{\partial \delta_2} = |V_1 V_2 Y_{21}|\, sin(\delta_1 - \delta_2 + \theta_{21}) \tag{3.7}$$

$$J_{12} = \frac{\partial f_{P_2}}{\partial V_2} = |V_1 Y_{21}|\, cos(\delta_1 - \delta_2 + \theta_{21}) + |2 V_2 Y_{22}|\, cos(\theta_{22}) \tag{3.8}$$

$$J_{21} = \frac{\partial f_{Q_2}}{\partial \delta_2} = |V_1 V_2 Y_{21}|\, cos(\delta_1 - \delta_2 + \theta_{21}) \tag{3.9}$$

$$J_{22} = \frac{\partial f_{Q_2}}{\partial V_2} = -|V_1 Y_{21}|\, sin(\delta_1 - \delta_2 + \theta_{21}) - |2V_2 Y_{22}|\, sin(\theta_{22}) \tag{3.10}$$

The aim of employing Newton-Raphson Equation 3.11 is to bring the solution of voltage magnitude and phase angle as close as possible to the true values by finding the roots of the mismatch equations. The Jacobian must be invertible for the solution to converge, meaning it cannot be singular or near-singular [4].

$$\begin{bmatrix} \delta_2 \\ V_2 \end{bmatrix}^{(n+1)} = \begin{bmatrix} \delta_2 \\ V_2 \end{bmatrix}^{(n)} - \boldsymbol{J}^{-1} \begin{bmatrix} f_{P_2} \\ f_{Q_2} \end{bmatrix} \tag{3.11}$$

This process is iterative, where the values for voltage magnitude and phase angle are updated for each iteration, the mismatch equations and the Jacobian matrix are recalculated, and the process is repeated until the mismatch function is minimized, meaning until the tolerance is achieved. The algorithm for the NR method was developed using MATLAB (See Appendix). The convergence tolerance was chosen to be reasonably small for the solutions to be accurate, $tolerance = 0.001$.

3.2 A Dynamic Model of the Two-Bus System

The aim with the dynamic model in state-space form is to examine the transient and steady-state response of the voltage magnitude and the phase angle at the second bus by changing active and reactive power values of the load. To achieve this, a dynamic model of the two-bus system based on the modified case4_dist model must be developed. The system must be converted from a balanced three-phase network into a single-phase circuit, as discussed in Section 2.3.

The transmission line is modeled as a π-model, as discussed in Section 2.7. A small value resistor, R_s, of 0.01 Ω is added to the circuit that represents the internal resistance of the voltage supply. Stray capacitance, between the transmission line and the ground, is represented by C_1 and C_2 and both values are $0.1\mu F/km$. The capacitance is chosen to be low, since the model is assumed to have transmission line length of $1km$ and the stray capacitance effect is assumed to be small when the system reaches steady-state. The capacitance value has an effect over the transient response that is discussed in the Section 4.3.

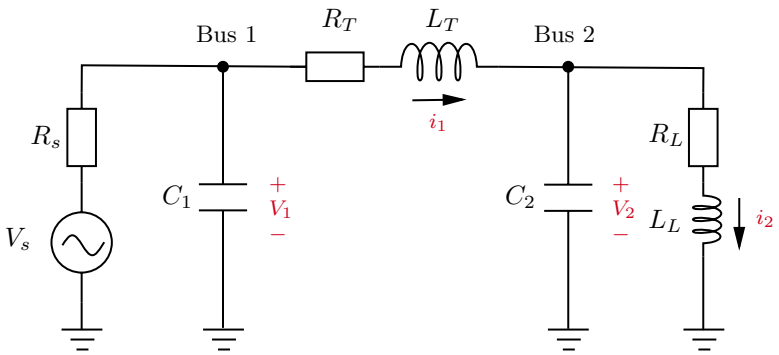

Figure 3.3: Single-phase diagram of a two-bus system

The rest of the system values specified in per unit in the case4_dist model must be converted to actual values. The transmission line reactance is $Z_{line} = 0.003 + j0.006$ pu. The resistive component is straightforwardly scaled by the impedance base value Z_b, discussed in Section 2.3. The inductances can be found through the inductive reactance, X_L, Equation 3.12, since the frequency, f is 50Hz. The actual values of R_T and L_T are $0.4688\Omega/km$ and $3mH/km$, respectively.

$$X_L = \omega L \tag{3.12}$$

The apparent power for load that is specified in the case4_dist model is $S_2 = P_2 + jQ_2 = 0.4 + j0.2$ pu for the three-phase network. By multiplying it with the apparent base value, S_b of 1 MVA and then scaling it down by a third, the value is converted to single-phase apparent power of the load. Load impedance, Z_{load} can then be calculated, as shown in Equation 2.5 (Section

2.3). With the load impedance known, the values for load resistance R_L and inductance L_L are calculated similarly as for the transmission lines. The actual load resistance R_L and inductance L_L are 312.5Ω and $497mH$, respectively.

The number of states in the system can be determined by the number elements that can store energy and affect the system's behaviour over time. Such passive elements are the capacitors and inductors that display time-dependent behaviour, as shown in Equations 3.13 and 3.14.

$$i = C\frac{dv}{dt} \tag{3.13}$$

$$v = L\frac{di}{dt} \tag{3.14}$$

The voltages across capacitors C_1 and C_2 and the current through inductors L_T and L_L are chosen as state variables, with the voltage supply V_s designated as the input. By applying Kirchhoff's voltage law (KVL) to the loops and Kirchhoff's current law (KCL) to the nodes of the circuit, linearly independent, first-order differential state Equations 3.15, 3.16, 3.19, and 3.20 are derived.

$$\frac{dV_1}{dt} = -\frac{1}{C_1R_s}V_1(t) - \frac{1}{C_1}i_1(t) + \frac{1}{C_1R_s}V_s(t) \tag{3.15}$$

$$\frac{di_1}{dt} = \frac{1}{L_T}V_1(t) - \frac{R_T}{L_T}i_1(t) - \frac{1}{L_T}V_2(t) \tag{3.16}$$

$$\frac{dV_2}{dt} = \frac{1}{C_2}i_1(t) - \frac{1}{C_2}i_2(t) \tag{3.17}$$

$$\frac{di_2}{dt} = \frac{1}{L_L}V_2(t) - \frac{R_L}{L_L}i_2(t) \tag{3.18}$$

The state variables are redefined and rewritten in a state vector form as follow:

$$\begin{bmatrix} x_1(t) \\ x_2(t) \\ x_3(t) \\ x_4(t) \end{bmatrix} = \begin{bmatrix} V_1(t) \\ i_1(t) \\ V_2(t) \\ i_2(t) \end{bmatrix} \tag{3.19}$$

The differential state equations can be rewritten in state-space form, as presented in Equations 3.20 and 3.21. The state matrix, $\boldsymbol{A}$, captures the intrinsic dynamics of the system, while the input matrix, $\boldsymbol{B}$ incorporates the scalar factor of the input signal. The state derivative vector is $\dot{\boldsymbol{x}}(\boldsymbol{t})$, vector of states is $\boldsymbol{x}(\boldsymbol{t})$, and $u(t)$ is the supply voltage, V_s that acts as input to the system. The state-space model is a linear time-invariant (LTI) system because the coefficients of the matrices are not time-dependent.

$$\begin{bmatrix} \dot{x}_1(t) \\ \dot{x}_2(t) \\ \dot{x}_3(t) \\ \dot{x}_4(t) \end{bmatrix} = \begin{bmatrix} -\frac{1}{C_1R_s} & -\frac{1}{C_1} & 0 & 0 \\ \frac{1}{L_T} & -\frac{R_T}{L_T} & -\frac{1}{L_T} & 0 \\ 0 & \frac{1}{C_2} & 0 & -\frac{1}{C_2} \\ 0 & 0 & \frac{1}{L_L} & -\frac{R_L}{L_L} \end{bmatrix} \begin{bmatrix} x_1(t) \\ x_2(t) \\ x_3(t) \\ x_4(t) \end{bmatrix} + \begin{bmatrix} \frac{1}{C_1R_s} \\ 0 \\ 0 \\ 0 \end{bmatrix} u(t) \tag{3.20}$$

For the output, the direct transmission matrix, $\boldsymbol{D}$ is zero. The output is defined to be the as the state variable $x_3(t)$ that is the voltage, V_2 since the goal is to find the voltage magnitude and the angle over the second bus, Equation 3.21.

$$y(t) = \begin{bmatrix} 0 & 0 & 1 & 0 \end{bmatrix} \begin{bmatrix} x_1(t) \\ x_2(t) \\ x_3(t) \\ x_4(t) \end{bmatrix} \tag{3.21}$$

The state-space system was solved using MATLAB (see Appendix) by performing a time-domain simulation to analyze the response of the linear system provided the input V_s and the following initial conditions: $x_1(t_0) = 0$, $x_2(t_0) = 0$, $x_3(t_0) = 0$, $x_4(t_0) = 0$. These initial conditions represent a de-energized state of the system at t_0. The input, V_s is sinusoidal (Equation 2.7) with a frequency of 50 Hz, scaled by the magnitude V_{peak} and the phase-shift $\theta = 0$.

As mentioned before, the state matrix, $\boldsymbol{A}$, describes the core dynamics of the two-bus system. It encapsulates the coefficients of the resistive (R_L) and inductive (L_L) components of the load connected at the second bus. By changing these values, it can be studied how they influence the voltage in the system.

3.3 Simscape Model of the Two-Bus System

A Simscape model of a simplified power system is shown in Figure 3.4. The system consist of two buses: swing (slack) bus and a PQ load. The slack is connected to solver configuration that specifies the parameters that the model needs, and a busbar that is connected to the transmission line. TThe transmission line is represented as π model whit one shunt capacitor at each end of the line. The second busbar is connected to the second bus, PQ load bus.

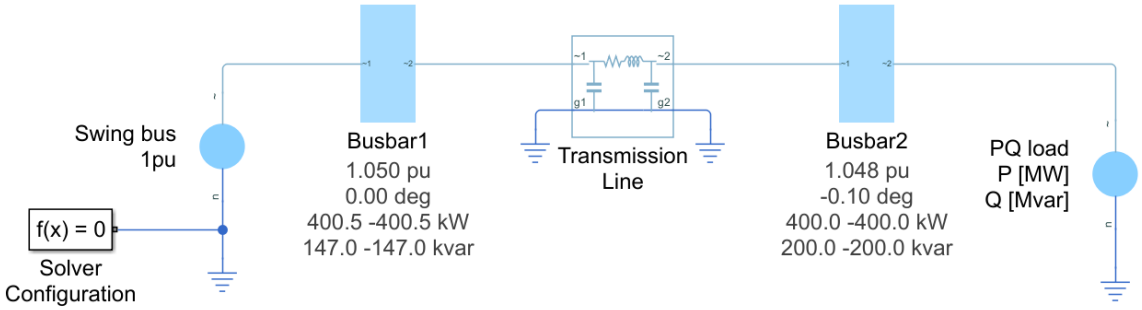

Figure 3.4: Simscape model of a two-bus system. Swing bus and PQ load bus are connected via the transmission line.

The power flows from the swing bus to the PQ load. The busbar has no effect on the dynamics of the system, it is just a MATLAB Simscape component that measure the voltage and phase values. It shows the values in pu basis as well as in kW for active power and kVAR for reactive power. This model was used to validate the results obtained trough the Newton-Raphson method, showing correct results and consistency.

3.4 A Dynamic Model of the Modified case4_dist Network

The objective with the state-space representation of the full modified case4_dist model is to assess the impact of changes in active and reactive power of a load on the bus voltage magnitudes. In other words, to study voltage sensitivities in the system.

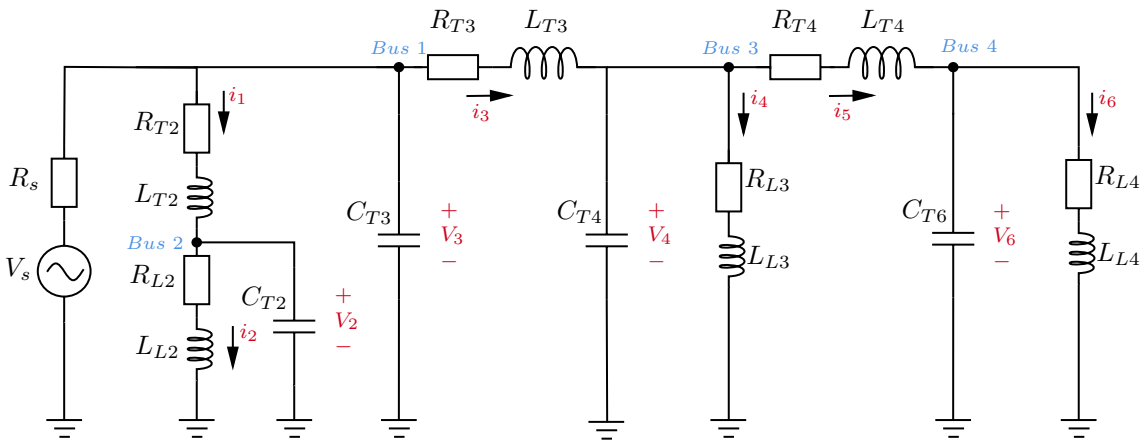

Figure 3.5: Single-phase diagram of the case4_dist model

The full single-phase equivalent circuit of the modified case4_dist model, presented in Section 2.2, is illustrated in Figure 3.4. The first bus is the slack bus, where the generator V_s with a small internal resistance R_s of 0.01 Ω is connected. The second, third and fourth buses are PQ buses, each with one load connected to it with identical apparent power demand value of $P = 0.4$ pu and $Q = 0.2$ pu.

The transmission lines can be modeled by cascading several π-model sections. The parallel shunt capacitances between the first and the second buses can be combined to form C_{T3}. The same applies to the shunt capacitances between the first and third buses, forming C_{T4}. The capacitance value for both C_{T2} and C_{T6} is $0.1\mu F/km$ and the value for both C_{T3} and C_{T4} is $0.1\mu F/km$. The the resistive components in the transmission lines have the same value: $R_{T2} = R_{T3} = R_{T4} = 0.4688\Omega/km$. The same applied for the line inductances: $L_{T2} = L_{T3} = L_{T4} = 3mH/km$. The reasoning of these values is discussed in Section 3.2. It assumed that the length of each $\pi - model$ section is 1 km.

Following the same reasoning as in Section 3.2, the chosen state variables are as follow: $x_1(t) = i_1$, $x_2(t) = V_2$, $x_3(t) = i_2$, $x_4(t) = V_3$, $x_5(t) = i_3$, $x_6(t) = V_4$, $x_7(t) = i_4$, $x_8(t) = i_5$, $x_9(t) = V_6$, $x_{10}(t) = i_6$. Applying KCL to the nodes and KVL to the loops, ten first-order linear, time-invariant differential equations (see Appendix) are obtained that describe the behaviour of the system. The equations are directly expressed in state-space form, in Equations 3.22, 3.23, 3.24, and 3.24. The state matrix, $\boldsymbol{A}$ has size 10×10 and encapsulates the coefficients that describe the systems dynamics. The input matrix $\boldsymbol{B}$ is of size 10×1 and describes how the input affects the states.

$$\boldsymbol{A} = \begin{bmatrix} \frac{-R_{T2}}{L_{T2}} & \frac{-1}{L_{T2}} & 0 & \frac{1}{L_{T2}} & 0 & 0 & 0 & 0 & 0 & 0 \\ \frac{1}{C_{T2}} & 0 & \frac{-1}{C_{T2}} & 0 & 0 & 0 & 0 & 0 & 0 & 0 \\ 0 & \frac{1}{L_{L2}} & \frac{-R_{L2}}{L_{L2}} & 0 & 0 & 0 & 0 & 0 & 0 & 0 \\ \frac{-1}{C_{T3}} & 0 & 0 & \frac{-1}{R_s C_{T3}} & \frac{-1}{C_{T3}} & 0 & 0 & 0 & 0 & 0 \\ 0 & 0 & 0 & \frac{1}{L_{T3}} & \frac{-R_{T3}}{L_{T3}} & \frac{-1}{L_{T3}} & 0 & 0 & 0 & 0 \\ 0 & 0 & 0 & 0 & \frac{1}{C_{T4}} & 0 & \frac{-1}{C_{T4}} & \frac{-1}{C_{T4}} & 0 & 0 \\ 0 & 0 & 0 & 0 & 0 & \frac{1}{L_{L3}} & \frac{-R_{L3}}{L_{L3}} & 0 & 0 & 0 \\ 0 & 0 & 0 & 0 & 0 & \frac{1}{L_{T4}} & 0 & \frac{-R_{T4}}{L_{T4}} & \frac{-1}{L_{T4}} & 0 \\ 0 & 0 & 0 & 0 & 0 & 0 & 0 & \frac{1}{C_{T6}} & 0 & \frac{-1}{C_{T6}} \\ 0 & 0 & 0 & 0 & 0 & 0 & 0 & 0 & \frac{1}{L_{L4}} & \frac{-R_{L4}}{L_{L4}} \end{bmatrix} \tag{3.22}$$

$$\boldsymbol{B} = \begin{bmatrix} 0 \\ 0 \\ 0 \\ \frac{1}{R_s C_{T3}} \\ 0 \\ 0 \\ 0 \\ 0 \\ 0 \\ 0 \end{bmatrix} \tag{3.23}$$

The output matrix $\boldsymbol{C}$, Equation 3.24, has size 10×4 and identifies the specific outputs that are monitored in the system. These outputs correspond to the bus voltage magnitudes. By structuring the output matrix in this form, bus voltages can be tracked individually at the same time. This approach helps to analyze how load variations impact the voltage stability and to study transient responses.

$$\boldsymbol{C} = \begin{bmatrix} 0 & 1 & 0 & 0 & 0 & 0 & 0 & 0 & 0 & 0 \\ 0 & 0 & 0 & 1 & 0 & 0 & 0 & 0 & 0 & 0 \\ 0 & 0 & 0 & 0 & 0 & 1 & 0 & 0 & 0 & 0 \\ 0 & 0 & 0 & 0 & 0 & 0 & 0 & 0 & 1 & 0 \end{bmatrix} \tag{3.24}$$

Each row in the output matrix $\boldsymbol{C}$ corresponds to one of the monitored bus voltages as follow:

- The first row captures the voltage at the second bus (V_2)
- The second row captures the voltage at the first bus (V_3)
- The third row captures the voltage at the third bus (V_4)
- The fourth row captures the voltage at the fourth bus (V_6)

The source V_s is the input signal $u(t)$ that is a sinusoidal wave with an angular frequency ω of 100π

Chapter 4

Results

The results obtained from the developed, two-bus and four-bus models, based on the modified case4_dist four-bus distribution network, are discussed. First, the performance comparison between solutions obtained through the Newton-Raphson method and the state-space model is examined. Following this, the voltage sensitivity of the four-bus system is analyzed and interpreted. Finally, the transient response is evaluated to understand the system's behaviour under dynamic conditions.

4.1 Comparative Analysis of Two-Bus Systems Using NR-Method and State-Space Model

The objective developing two simplified two-bus representations from the case4_dist model is to assess the performance of Newton-Raphson (NR) approach against the dynamic model in State-Space, which are introduced in Sections 3.1 and 3.2.

The power flow equations, that describe the power flow within a balanced distribution network, are static. They represent the steady-state conditions of the system. The common approach is to manipulate and solve these equations by NR method to find the voltage magnitudes and phase angles in all the buses of a distribution network. However, it does not account for dynamic analysis or the transient effects. This is where a dynamic a model of the system becomes desirable, but it needs to be determined if the dynamic model performs as effectively as the NR method in providing steady-state solutions. The aim was to conduct a comprehensive comparison and evaluate the degree of similarity between the steady-state solutions produced by these two approaches.

The approach taken for the two-bus system model involves generating random apparent power values, S_2, for the load connected to the second bus (Figure 3.1), ranging from 0.1 pu to 2 pu. These values were randomly assigned to active and reactive power of the load, and sorted in increasing order. This ordering of values helps with clear plotting and interpretation of the results and it does not affect the outcome otherwise. This same technique was employed for dynamic state-space model with the involved conversions from per unit basis of active and reactive power to resistive and inductive values of the load (Figure 3.3), discussed in Section 3.2.

To compare the performance of both methods, twenty different apparent power load values were generated. For each model, the resulting steady-state voltage magnitudes (in kilovolts) and their corresponding phase angles values (in degrees) are plotted on the x-axis [kV] and y-axis [deg], respectively. This is illustrated in Figure 4.1.

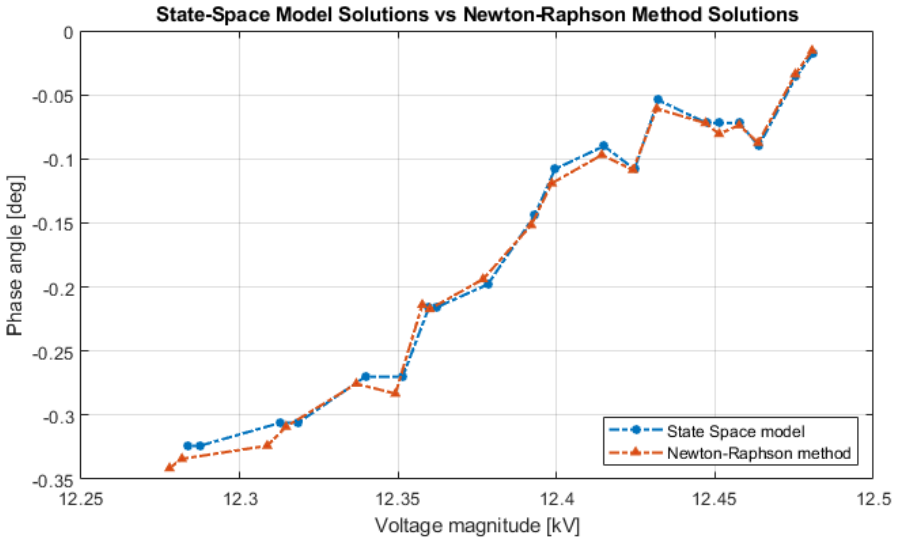

Figure 4.1: Solution Comparison: Newton-Raphson Method and State-Space Model

The orange dotted line corresponds to the solutions obtained through Newton-Raphson method while the blue dotted line are the solutions for state-space model. The values of active and reactive power were applied to the models in increasing order, the resistivity and inductivity of the load values gradually increased. The plot meets the expectations, showing that the values of magnitude and phase angle decrease. For the first solution, the voltage magnitude is around 12.5 kV and the phase angle is around 0 degrees. With each increase in the load's apparent power the resulting voltage magnitude and phase angle are decrease. Both models are closely aligned and follow approximately the same trend. Although the models may appear to have some discrepancies, they are quite small. This is illustrated in Table 4.1, where the last ten values from the graph are shown, as this is where the difference between the trends appears to be the largest.

Table 4.1: Comparison of voltage and phase angle values between measured at bus number two obtained through Newton-Raphson method and the state space model

$S_{load} = P_2 + jQ_2$	NR algorithm	State Space model	Discrepancy
$S = 0.921 + j0.967$	$12.39kV \angle -0.15°$	$12.39kV \angle -0.14°$	$0.00kV \angle 0.01°$
$S = 1.097 + j1.077$	$12.38kV \angle -0.19°$	$12.38kV \angle -0.20°$	$0.00kV \angle 0.01°$
$S = 1.237 + j1.226$	$12.36kV \angle -0.22°$	$12.36kV \angle -0.22°$	$0.00kV \angle 0.00°$
$S = 1.242 + j1.254$	$12.36kV \angle -0.21°$	$12.36kV \angle -0.22°$	$0.00kV \angle 0.01°$
$S = 1.445 + j1.262$	$12.35kV \angle -0.28°$	$12.35kV \angle -0.27°$	$0.00kV \angle 0.01°$
$S = 1.491 + j1.400$	$12.34kV \angle -0.28°$	$12.34kV \angle -0.27°$	$0.00kV \angle 0.01°$
$S = 1.682 + j1.592$	$12.31kV \angle -0.31°$	$12.32kV \angle -0.31°$	$0.01kV \angle 0.00°$
$S = 1.746 + j1.636$	$12.31kV \angle -0.32°$	$12.31kV \angle -0.31°$	$0.00kV \angle 0.01°$
$S = 1.906 + j1.903$	$12.28kV \angle -0.33°$	$12.29kV \angle -0.32°$	$0.01kV \angle 0.01°$
$S = 1.943 + j1.935$	$12.28kV \angle -0.34°$	$12.28kV \angle -0.32°$	$0.00kV \angle 0.02°$

Table 4.1 displays the randomly generated apparent power load values in per unit. The corresponding results values for the Newton-Raphson method and state-space model are presented. The last column shows the difference in voltage magnitude and the phase angle between the NR algorithm and the state-space model. The maximum difference is 0.01 kV for voltage magnitude and 0.02° for the phase angle. The small discrepancy may be due to numerical inaccuracies in the Newton-Raphson method. These minimal differences indicate that the dynamic model performs

comparably to the NR method.

By keeping the active power constant and gradually increasing the reactive power by generating random numbers in the interval of 0.1 pu to 2 pu, it is possible to observe how the increase in load reactive power affect the bus voltage and angle. The results are shown in the Figure 4.2. Both methods display approximately the same trend. At the second bus, the voltage magnitude drops from around 12.47kV to 12.35kV as the load reactive power varies from 0.1 pu to 2 pu. This voltage drop is expected since the increase in loads reactive power increases the loads impedance, resulting in voltage drop. The inductive component causes the phase angle to shift in the positive direction, moving from around -0.11° to 0.11°. This shift occurs because increased reactive power leads to higher inductance, which affects the phase angle. Both models exhibit similar trends, indicating accurate solutions.

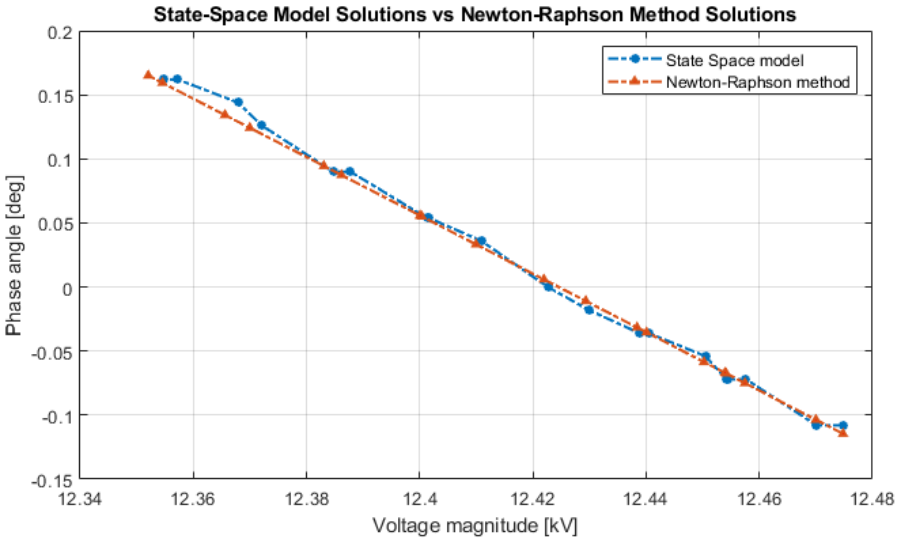

Figure 4.2: Solution Comparison: Keeping the active power constant

Similarly, Figure 4.3 the results with the reactive power kept constant. As the active power is increased the voltage magnitude decreases and the phase angle shifts in the negative direction, moving from 0° to -0.55°. The consistent alignment between the resulting trends indicate reliable and accurate results.

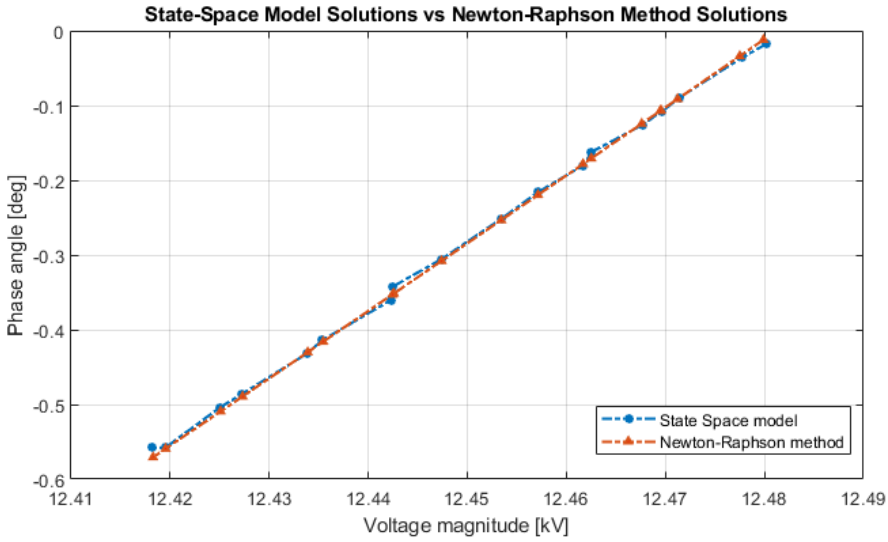

Figure 4.3: Solution Comparison: Keeping the reactive power constant

One observation that was made when generating transient data with the state-space model is that due to high frequencies in the transient, a high sampling of 100 kHz was required to get achieve a proper resolution. This increased the simulation time. It

In summary, the comparison of the models indicates that the the dynamic model produces results comparable to those of the Newton-Raphson method. The two-bus model validates the effectiveness of the dynamic model, showing that is performs nearly as well as the NR method.

4.2 Voltage sensitivity analysis for the modified case4_dist model

The voltage sensitivity analysis helps to understand how a change in load power consumption affects the voltage magnitudes at the buses in the system. To perform this analysis, a change in load apparent power was applied to the full dynamic model (Figure 3.3), based on modified case4_dist model (Figure 2.3), after the system had reached a steady-state condition.

The initial load at the fourth bus is 0.447 MVA, which is 44.7% of the base power. Then, the load is increased to 100% of the base power when the system reaches steady-state. This value is still within the limits of the base power capacity of 1 MVA. It represents a substantial increase of 122% in apparent power consumption at bus four. This increase will produce a voltage drop at other buses, which are summarized in Table 4.2

Table 4.2: Voltage Sensitivity Analysis for the Four-Bus Dynamic Model

Bus Voltage	$\boldsymbol{S_4 = P_4 + jQ_4}$ **0.4+j0.2**	$\boldsymbol{S_4 = P_4 + jQ_4}$ **0.8+j0.6**	**Relative Voltage Drop as a Percentage**
$\boldsymbol{V_1}$	$12.50kV$	$12.50kV$	0
$\boldsymbol{V_2}$	$11.74kV$	$11.74kV$	0
$\boldsymbol{V_3}$	$11.72kV$	$11.68kV$	0.34
$\boldsymbol{V_4}$	$11.69kV$	$11.60kV$	0.77

The first column in the Table 4.2 indicates the bus to which the voltage values correspond. The second column shows the respective voltages at the initial load with an apparent power of, $S_4 = 0.4 + j0.2$. The voltage at the first bus remains unchanged, as expected, since this is the slack bus. All buses are radially connected (Figure 2.3), meaning there is a single path for each bus to reach the source. The second bus is connected to a different branch than the third and fourth buses. This explains the higher starting voltage value at the second bus of 11.74kV compared to the third and fourth buses, which have starting values of 11.72kV and 11.69kV, respectively.

After the increase in load's apparent power, there is a voltage drop at buses three and four, as presented in the second column, since they are connected to the same branch. The relative voltage change for each bus is summarized in the fourth column as voltage drop in percentage . As expected, the slack bus voltage presents no change, and the second bus voltage remains unaffected since it is connected to a different branch. The fourth bus shows the highest voltage drop of 0.77%, where the load change occurs. The third bus has a lower voltage drop of 0.34% , illustrating how the changes in load can affect voltage values in other parts of the distribution systems.

To make sense if this voltage variation is within reasonable level, the Norwegian Regulation on Delivery Quality and Power Systems provides a standard. According to a statute (FOR-1990-12-07-959-§3-3, 2004) issued by "Norwegian Ministry of Petroleum and Energy", it states: *"§ 3-3. Slow variations in the effective value of the voltage: The grid company shall ensure that slow variations in the effective value of the voltage are within a range of* $\pm 10\%$ *of the nominal voltage, measured as an average over one minute, at the connection point in the low voltage network"*[15]

A variation of $\pm 10\%$ of the nominal value is accepted for a local distribution grid. Figure 4.4 shows four graphs where the alternating bus voltage V_i is plotted with the source voltage, V_s (i.e., the slack bus voltage) over time for each bus in the network. By comparing the peak values at the last crest of the sinusoidal wave of the voltage source and the bus voltage, at around 0.07 seconds, when the system has reached steady state, it is possible to calculate the voltage drop. This is

presented in Table 4.3, where the first column displays the bus number, the second column shows the voltage magnitude and the phase angle of each bus, and the third column shows the voltage drop as a percentage, comparing the source voltage magnitude with the bus voltage magnitude.

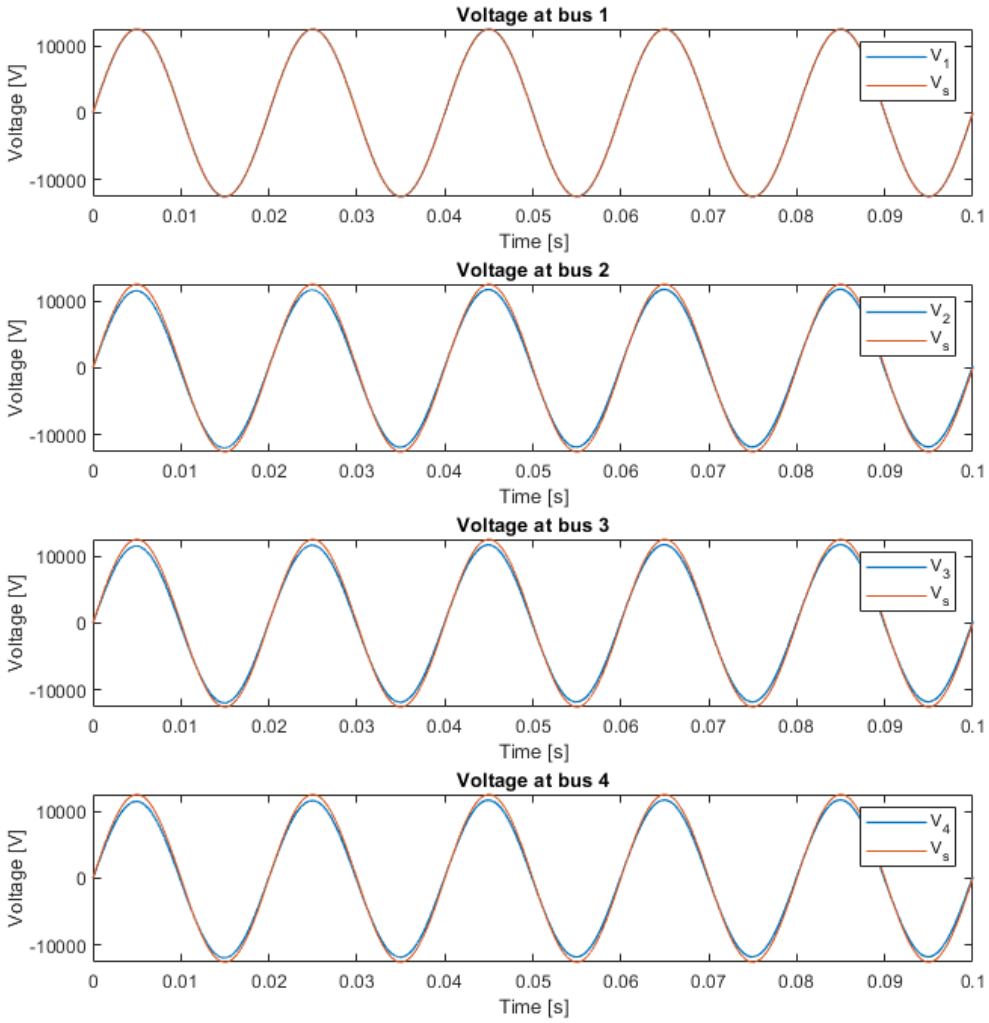

Figure 4.4: Simulated Voltage Responses at Four Buses of case4_dist State-Space Model

The voltage drop lies around 6% with the highest voltage drop being at the fourth bus of 6.6%. Adding the highest voltage change of 0.77% for the fourth bus from table 4.2, it results in a total of **7.37%**, which is well within the ±10% threshold stated in the regulation.

In summary, the developed dynamic model allows to monitor and interpret the voltage sensitivities that occurs in the distribution network. The results allows for a clear understanding for how much the different buses in the system are affected by a load change in a specific part of the system. Although the phase angles were not used for this analysis, it is illustrated in table 4.3 that the angles can be extrapolated from the phase difference between the source wave and the bus voltage wave by taking the time difference.

Table 4.3: Voltage Drop Analysis for Each Bus in the Dynamic Model

Bus number	$\|V\| \angle\phi$	**Voltage drop with respect to slack bus voltage**
1	$12.50kV \angle 0.072$	0%
2	$11.74kV \angle 1.368$	6%
3	$11.72kV \angle 1.224$	6.24%
4	$11.69kV \angle 1.062$	6.48%

4.3 Transients Response and Steady-State Analysis

One of the many benefits of the dynamic model over the static model is that it provides information about transients. The dynamic model of the two-bus system presented in Section 3.2 (Figure 3.3) was used to analyze the transient response with two different but equivalent input sources: sinusoidal wave AC and the DC equivalent, V_{rms}. The graphs show the voltage results for a single-phase system. This is fine for the transient response interpretation, because the system is assumed to be balanced.

At the start of the simulation, all initial values are set to zero. This simulates a de-energized state of the system and produces a transient when the system is "energized". Figures 4.5 and 4.6 show the transient response of the two-bus dynamic model for each input source used. The first plot (Figure 4.5) shows voltage variation at the second bus, V_2 with the input AC source signal V_s with a peak value of $10,2kV$. The transient is embedded into the resulting voltage V_2. A close-up of the crest is illustrated in (Figure 4.6) for the first 0.001 seconds, where the ripples in V_2 are present. Voltage difference between the ripples is at most of around 60V.

To get a better understanding of what is happening and how fast the voltage is converging to its nominal value, an equivalent response was simulated with the RMS voltage V_{rms} as the input source. This is illustrated in the second plot of Figure 4.5. The resulting response at the second bus V_2 is plotted together with V_{rms}. Very short convergence time of around 0.05s can be observed, which is typical for electrical systems. High frequency fluctuations are present shown in the second plot in Figure 4.6 in a close-up. These fluctuations reach voltage values way above the nominal value of 7,2kV, V_{rms}, but it does not directly translate to the real voltage levels in the system, since the source is AC and the transient is embedded in the response.

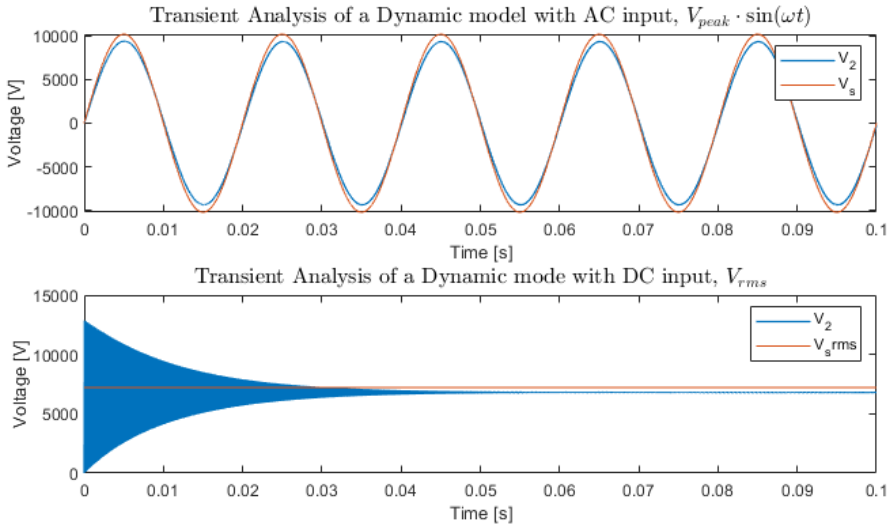

Figure 4.5: Transient Response of the Two-Bus System

In summary, these results show a very short convergence times of the transient, in order of

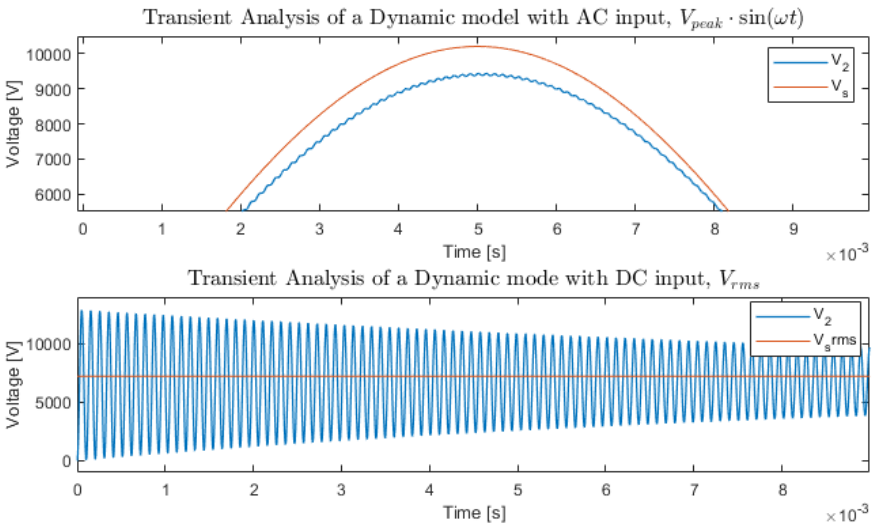

Figure 4.6: Transient Response Embedded into the Sinusoidal Signal

milliseconds, and the effects that this has on the resulting output wave. The analysis highlights the importance of accurately modeling transient responses to ensure the stability and reliability of power systems, particularly when integrating renewable energy sources. Future work could explore more sophisticated models, consider additional factors such as harmonics and investigate the impact of varying load conditions.

Chapter 5

Conclusion

The dynamic model shows minimal solution discrepancies compared to the solutions obtained through power flow equations that were solved using the iterative Newton-Raphson (NR) method. This indicates that the model is reliable for assessing voltage stability analysis of the distribution network. Additionally, it provides a means to evaluate how changes in one part of the system affect the rest of the system, and allows to conduct voltage a straightforward sensitivity analysis.

State-space representation offers several advantages over static equations and iterative methods, such as transients response analysis, simultaneous assessment of all bus voltages, and improved processing performance. It also avoids the solution divergence issues that can occur applying the NR method. One disadvantage compared to the Newton-Raphson method is that if the system changes, the state matrix requires a to be updated, and potentially new states introduced which requires the reevaluation of the dynamics of the system. For large systems, a well-defined dynamic model can improve the computational cost compared to Newton-Raphson method, since it does not require recalculating the system matrices to converge to a solution.

This thesis demonstrates the potential of dynamic models for real distribution networks. The approach is scalable, can improve monitoring of the network, and helps to mitigate the challenges, such as voltage variability, from the integration of renewable energy sources in the grid.

As future work, the model can be increased in complexity, and control techniques such as state feedback or observer-based control can be implemented for voltage control. For real-time monitoring, fault detection and noise reduction in the data, the implementation of Kalman filter is proposed to estimate the states in the system for better monitoring and control of the power distribution system.

Bibliography

[1] European Environment Agency. Share of energy consumption from renewable sources. https://www.eea.europa.eu/en/analysis/indicators/share-of-energy-consumption-from. Accessed: 2024-06-05.

[2] Göran Andersson. Modelling and analysis of electric power systems. *ETH Zurich*, pages 5–6, 2008.

[3] Tobias Blenk and Christian Weindl. Fundamentals of state-space based load flow calculation of modern energy systems. *Energies*, 16(13):4872, 2023.

[4] Kheelesh Kumar Dewangan and Ashish K Panchal. Power flow analysis using successive approximation and adomian decomposition methods with a new power flow formulation. *Electric Power Systems Research*, 211:108190, 2022.

[5] Savo D Dukic and Andrija T Saric. Dynamic model reduction: An overview of available techniques with application to power systems. *Serbian journal of electrical engineering*, 9(2):131–169, 2012.

[6] Energidepartementet. Norway's energy supply system. Statnett SF, the electricity grid. https://energifaktanorge.no/en/norsk-energiforsyning/kraftnett/#:~:text=The%20Norwegian%20electricity%20grid%20consists,as%20defined%20by%20EU%20legislation., 2024. Accessed: 2024-02-03.

[7] Eurostat. Share of energy consumption from renewable sources. https://ec.europa.eu/eurostat/databrowser/view/nrg_ind_ren/default/table?lang=en. Accessed: 2024-06-05.

[8] Mirko Ginocchi, Ferdinanda Ponci, and Antonello Monti. Sensitivity analysis and power systems: Can we bridge the gap? a review and a guide to getting started. *Energies*, 14(24):8274, 2021.

[9] Ogata Katsuhiko. *Modern control engineering*. Editorial Félix Varela, 2009.

[10] Prabha Kundur. Power system stability. *Power system stability and control*, 10:7–1, 2007.

[11] Kenneth Lange and Kenneth Lange. Singular value decomposition. *Numerical analysis for statisticians*, pages 129–142, 2010.

[12] Xinyu Liang, Hua Chai, and Jayashri Ravishankar. Analytical methods of voltage stability in renewable dominated power systems: a review. *Electricity*, 3(1):75–107, 2022.

[13] Federico Milano. *Power Flow Analysis*, pages 61–101. Springer Berlin Heidelberg, Berlin, Heidelberg, 2010.

[14] James W Nilsson and Susan Riedel. *Electric circuits*. Prentice Hall Press, 2010.

[15] Olje og energidepartementet. Forskrift om leveringskvalitet i kraftsystemet., 2004. FOR-2004-11-30-1557, FOR-1990-12-07-959-§7-1, LOV-1990-06-29-50-§7-6.

[16] Subhasis Panda, Sarthak Mohanty, Pravat Kumar Rout, Binod Kumar Sahu, Shubhranshu Mohan Parida, Hossam Kotb, Aymen Flah, Marcos Tostado-Véliz, Bdereddin Abdul Samad, and Mokhtar Shouran. An insight into the integration of distributed energy resources and energy storage systems with smart distribution networks using demand-side management. *Applied Sciences*, 12(17):8914, 2022.

[17] Allen J Wood, Bruce F Wollenberg, and Gerald B Sheblé. *Power generation, operation, and control*. John Wiley & Sons, 2013.

[18] Cheng Yang, Yupeng Sun, Yujie Zou, Fei Zheng, Shuangyu Liu, Bochao Zhao, Ming Wu, and Haoyang Cui. Optimal power flow in distribution network: A review on problem formulation and optimization methods. *Energies*, 16(16):5974, 2023.

Appendix A

Impedance

$$Z = R + jX = R + j(X_L - X_C)$$

Admittance

$$Y = \frac{1}{Z} = G - jB = G + j(B_C - B_L)$$

Pure inductance

$$Y = -jB_L$$

Instantaneous power (time domain)

$$p(t) = v(t)i(t)$$
$$p(t) = V_{\text{Peak}} \cos(\omega t + \delta) \cdot I_{\text{Peak}} \cos(\omega t + \beta)$$
$$p(t) = V_{\text{RMS}}\ I_{\text{RMS}} \cos(\delta - \beta)[1 + \cos(2\omega t + 2\delta)] + V_{\text{RMS}}\ I_{\text{RMS}} \sin(\delta - \beta) \sin(2\omega t + 2\delta)$$
$$I_R = I_{\text{RMS}} \cos(\delta - \beta)$$
$$I_X = I_{\text{RMS}} \sin(\delta - \beta)$$

Active power

$$P = V_{\text{RMS}} I_R$$

Reactive power

$$Q = V_{\text{RMS}} I_X$$

Complex power (phasor domain)

$$\boldsymbol{S} = \boldsymbol{V}\boldsymbol{I}^* = V_{\text{RMS}} I_{\text{RMS}} \angle(\delta - \beta)$$

Apparent power

$$\boldsymbol{S} = \boldsymbol{V}\boldsymbol{I}^* = V_{\text{RMS}} I_{\text{RMS}} = P + jQ$$

Expanded Jacobian matrix for a n-bus system:

$$\begin{bmatrix} \Delta P_2 \\ \vdots \\ \Delta P_n \\ \Delta Q_2 \\ \vdots \\ \Delta Q_n \end{bmatrix} = \begin{bmatrix} \frac{\partial P_2}{\partial \delta_2} & \cdots & \frac{\partial P_2}{\partial \delta_n} & \frac{\partial P_2}{\partial |V_2|} & \cdots & \frac{\partial P_2}{\partial |V_n|} \\ \vdots & \ddots & \vdots & \vdots & \ddots & \vdots \\ \frac{\partial P_n}{\partial \delta_2} & \cdots & \frac{\partial P_n}{\partial \delta_n} & \frac{\partial P_n}{\partial |V_2|} & \cdots & \frac{\partial P_n}{\partial |V_n|} \\ \frac{\partial Q_2}{\partial \delta_2} & \cdots & \frac{\partial Q_2}{\partial \delta_n} & \frac{\partial Q_2}{\partial |V_2|} & \cdots & \frac{\partial Q_2}{\partial |V_n|} \\ \vdots & \ddots & \vdots & \vdots & \ddots & \vdots \\ \frac{\partial Q_n}{\partial \delta_2} & \cdots & \frac{\partial Q_n}{\partial \delta_n} & \frac{\partial Q_n}{\partial |V_2|} & \cdots & \frac{\partial Q_n}{\partial |V_n|} \end{bmatrix} \begin{bmatrix} \Delta \delta_2 \\ \vdots \\ \Delta \delta_n \\ \Delta |V_2| \\ \vdots \\ \Delta |V_n| \end{bmatrix} \tag{1}$$

Jacobian of power flow equations for diagonal and off diagonal terms for

$\boldsymbol{J_{P\delta}}$:

1. Diagonal term

$$\frac{\partial P_i}{\partial \delta_i} = \sum_{\substack{k=1 \\ k \neq i}}^{n} |V_i||V_k| \left(-G_{ik} sin(\delta_i - \delta_k) + B_{ik} cos(\delta_i - \delta_k)\right)$$

2. Off-diagonal term

$$\frac{\partial P_i}{\partial \delta_k} = \sum_{\substack{k=1 \\ k \neq i}}^{n} |V_i||V_k| \left(G_{ik} sin(\delta_i - \delta_k) - B_{ik} cos(\delta_i - \delta_k)\right)$$

$\boldsymbol{J_{P|V|}}$:

1. Diagonal term

$$\frac{\partial P_i}{\partial |V_i|} = 2|V_i| \, G_{ii} + \sum_{\substack{k=1 \\ k \neq i}}^{n} |V_k| \left(G_{ik} cos(\delta_i - \delta_k) + B_{ik} sin(\delta_i - \delta_k)\right)$$

2. Off-diagonal term

$$\frac{\partial P_i}{\partial |V_k|} = \sum_{\substack{k=1 \\ k \neq i}}^{n} |V_i| \left(G_{ik} cos(\delta_i - \delta_k) + B_{ik} sin(\delta_i - \delta_k)\right)$$

$\boldsymbol{J_{Q\delta}}$:

1. Diagonal term

$$\frac{\partial Q_i}{\partial \delta_i} = \sum_{\substack{k=1 \\ k \neq i}}^{n} |V_i||V_k| \left(G_{ik} cos(\delta_i - \delta_k) + B_{ik} sin(\delta_i - \delta_k)\right)$$

2. Off-diagonal term

$$\frac{\partial Q_i}{\partial \delta_k} = \sum_{\substack{k=1 \\ k \neq i}}^{n} |V_i||V_k| \left(-G_{ik} cos(\delta_i - \delta_k) - B_{ik} sin(\delta_i - \delta_k)\right)$$

$\boldsymbol{J_{Q|V|}}$:

1. Diagonal term

$$\frac{\partial Q_i}{\partial |V_i|} = -2|V_i|\, B_{ii} + \sum_{\substack{k=1 \\ k \neq i}}^{n} |V_k| \left(G_{ik} sin(\delta_i - \delta_k) - B_{ik} cos(\delta_i - \delta_k)\right)$$

2. Off-diagonal term

$$\frac{\partial Q_i}{\partial |V_k|} = \sum_{\substack{k=1 \\ k \neq i}}^{n} |V_i| \left(G_{ik} sin(\delta_i - \delta_k) - B_{ik} cos(\delta_i - \delta_k)\right)$$

Base:

$$S_B = 1MVA = 10^6 VA$$
$$V_B = 12.5kV = 12500V$$
$$Z_B = \frac{V_B^2}{S_B} = 156.25\Omega$$
$$I_B = \frac{S_B}{V_B} = 80A$$

Values:

$$Z_{line} = Z_{line,pu} * Z_B = (0.003 + j0.006) * 156.25 = 0.46875 + j0.9375\Omega$$
$$Z_{load} = Z_{load,pu} * Z_B = (0.4 + j0.2) * 156.25 = 62.5 + j31.25\Omega$$
$$S_{generator} = S_{generator,pu} * S_B = (0.4 + j0.2) * 10^6 = 400kW + j200kVAR$$

$$Z = R + jX\Omega$$
$$X_L = \omega * L$$
$$\omega = 2\pi * 50Hz = 100\pi$$
$$LOAD : L_L = \frac{31.25}{100\pi} = 99.4mH$$
$$TRANSM.LINE : L_T = \frac{0.9375}{100\pi} = 2.98mH$$

CHAPTER 4.2

$$|S_4| = \sqrt{0.4^2 + 0.2^2} \approx 0.46MVA \tag{2}$$

$$|S_4| = \sqrt{0.8^2 + 0.6^2} = 1MVA \tag{3}$$

$$\frac{1MVA - 0.45MVA}{0.45MVA} = 1.22 * 100 = 122\% \tag{4}$$

Appendix B

Table of Contents


```
function [solution] = evaluateNRModel(S_input)
% Apparent power (Sb) and voltage (Vb) base
S_base = 1e6;                % Base apparent power
V_base = 12.5e3;             % 3-phase RMS voltage value = base voltage val.
Z_base = (V_base^2)/S_base; % Base impedance = 156.25ohm

% System parameters
S_pu = S_input;              % Apparent on load side in [p.u.]
p2_pu = -1*real(S_pu);       % Active pwr, P. Negative = load consum. pwr
q2_pu = -1*imag(S_pu);       % Reactive pwr, Q. Negative = load consum. pwr
v1_pu = 1.0;                 % Voltage in [pu] at bus #1
d1 = 0;                      % Angle in [rad] at bus #1
Z_line_pu = 0.003+j*0.006;  % Transmission line impedance given in p.u.
%Y_line_pu = 1/Z_line_pu;    % Line admittance in [pu]

% The NR-method converges to a solution from the initial guess.
v2_pu = 1;               % Initial guess of voltage in [pu] at bus #2
d2 = 0;                  % Initial angle guess in [rad] at bus #2

% Converting from [pu] to actual values
Z_line = Z_line_pu * Z_base;     % Line impedance
Y_line = 1/Z_line;               % Line admittance
v1 = v1_pu * V_base;             % Voltage at bus #1
v2 = v2_pu * V_base;             % Voltage at bus #2
p2 = p2_pu * S_base;             % Active power at load bus
q2 = q2_pu * S_base;             % Reactive power at load bus

% Y bus matrices of magnitude and angle
Y = ones(2,2)*abs(Y_line);              % Y bus matrix of admittance mag.
Th = [angle(Y_line) angle(-Y_line);
      angle(-Y_line) angle(Y_line)];    % Y bus matrix of angles [rad]


% Jacobian matrix
J = zeros(2,2);     % Initialized J matrix for linearized PF equations

% Initial guess vector
X = [d2; v2];

% Loop parameters
iter = 0;                    % Tracks the number of complete iterations
tolerance = 1e-3;            % Final solution tolerance.
tolerance_achieved = false; % Stops the loop when the tolerance is achieved

% NR-method
while(~tolerance_achieved)
% Power flow equations
```

```
fp2 = abs(v1*v2*Y(2,1))*cos(d1-d2+Th(2,1))+abs(v2^2*Y(2,2))*cos(Th(2,2))-p2;
fq2 = -abs(v1*v2*Y(2,1))*sin(d1-d2+Th(2,1))-abs(v2^2*Y(2,2))*sin(Th(2,2))-q2;
fx = [fp2, fq2];

% Jacobian matrix populated with linearized power flow equations
J(1,1) = abs(v1*v2*Y(2,1))*sin(d1-d2+Th(2,1));
J(1,2) = abs(v1*Y(2,1))*cos(d1-d2+Th(2,1))+abs(2*v2*Y(2,2))*cos(Th(2,2));
J(2,1) = abs(v1*v2*Y(2,1))*cos(d1-d2+Th(2,1));
J(2,2) = -abs(v1*Y(2,1))*sin(d1-d2+Th(2,1))-abs(2*v2*Y(2,2))*sin(Th(2,2));

% NR-method: Calculating the next voltage and angle vector value
X = X - J\fx';

% Evaluating if the tolerance is good enough for solution convergence
toler_d2 = d2-X(1);     % Angle tolerance
toler_v2 = v2-X(2);     % Voltage tolerance
if (abs(toler_d2) < tolerance) && (abs(toler_v2) < tolerance)
    tolerance_achieved = true;  % Exit the loop
end

% Updating solution vectors and iteration.
v2 = X(2);
d2 = X(1);
iter = iter + 1;
end

% Converged solution
solution.v2 = v2*1e-3;          % In [kV]
solution.d2 = rad2deg(d2);      % In [degrees]

end
```

```
Error using evalin
Unrecognized function or variable 'evaluateNRmethod'.
```

Published with MATLAB® R2023b

Table of Contents


```
function [solution, graph] = evaluateSSModel(S_input, sampling)
%{
******************************************************
Purpose:
    Simulate a DC equivalent, expressed in state space,
    of a two bus system  and compare the output voltage
    and phase angle against a sinusoidal input.

Author:
    Kestutis Samulis, Mai 24, 2024
******************************************************
%}

f = 50;                                 % Frequency
w = 2*pi*f;                             % Angular frequency [rad/s]

% Specified base values
S_base = 1e6;                           % S_base [VA] is specified for a 3-phase
system.
V_base = 12500;                         % V_base [V] is the RMS voltage
specified for a 3-phase system.

% 3-phase RMS voltage
V_3phs_rms = V_base;                    % Base voltage is the RMS value of a
3-phase system
V_1phs_rms = V_3phs_rms/sqrt(3);        % Converting 3-phase rms voltage to
single-phase voltage

% Converting 3-phase apparent power to single-phase
%S_pu = 0.1 + j*0.1;                      % Apparent power delivered to load in
p.u. base.
S_pu = S_input;                         % Apparent power delivered to load in
p.u. base.
S_3phs_actual = S_pu*S_base;            % Converting p.u. value to actual value
for a 3-phase system.
S_1phs_actual = S_3phs_actual/3;        % Conveting the 3-phase apparent power
to single-phase apparent power.

% Finding load impedance
Z_load = (V_1phs_rms^2)/S_1phs_actual;

% Specified values for circuit components
C1 = 1e-7;                  % Capacitor in parallel with RS and RT
C2 = 1e-7;                  % Capacitor in parallel with LT and RL
Rs = 0.01;                  % Resistor in series with the voltage source
RT = 0.4688;                % Transmission line resistor
LT = 0.003;                 % Transmission line inductor
```

```
RL = real(Z_load);        % Load resistor
LL = -imag(Z_load)/w;     % Load inductor

% State space model of the two bus system
A = [ -1/(C1*Rs)     -1/C1        0        0;
       1/LT          -(RT/LT)    -1/LT     0;
       0             1/C2         0       -1/C2;
       0             0            1/LL     -(RL/LL)];
B = [1/(C1*Rs); 0;  0;  0];
C = [0 0 1 0];
D = 0;

% Sampling time
Fs = sampling.Fs;  % Sampling frequency
t0 = sampling.t0;  % Initial time
tf = sampling.tf;  % Final time
dt = 1/Fs;         % Time step
ts = t0:dt:tf;     % Sampling time

% Voltage magnitude is converted to peak voltage for single-phase
V_3phs_peak = V_3phs_rms * sqrt(2);   % Peak voltage of a 3-phase system
V_1phs_peak = V_3phs_peak/sqrt(3);    % Converting peak voltage from 3-phase
to single-phase


u = V_1phs_peak * sin(w*ts);          % Single-phase input voltage
oscillating sinusoidally

sys = ss(A, B, C, D);

% State initial condition
x0 = [0;0;0;0];

% Simulate system's output behaviour to the applied input voltage
[y, t] = lsim(sys, u, ts, x0);

% Sinusoidal input and ouput voltages with V_peak_1phs as magnitude
graph.t = t;
graph.u = u;
graph.y = y;


% Finding the peaks of input, u, and ouput, y, signals
[~, locs_u] = findpeaks(u, t);
[pks_y, locs_y] = findpeaks(y, t);

% Making sure that the same number of peaks is used in each case
locs_u = locs_u(end);   % Peak at steady state for u
locs_y = locs_y(end);   % Peak at steady state for y

% Calculating the average time difference
time_diff = locs_u - locs_y;

% Make sure that the angle is not hire than 90 degrees
```

```
phase_shift_rad = (w*time_diff);
phase_shift_deg = rad2deg(phase_shift_rad);
if abs(phase_shift_deg) > 90
    if phase_shift_deg < 0
        phase_shift_deg = -1*(phase_shift_deg+180);
    else
        phase_shift_deg = -1*(phase_shift_deg-180);
    end
end

% Converting voltage back from single-phase to 3-phase value.
V_peak_1phs     = pks_y(end);
V_peak_3phs     = V_peak_1phs*sqrt(3);
V_rms_3phs      = V_peak_3phs/sqrt(2);
V_rms_3phs_kV   = V_rms_3phs*1e-3;       % [V] to [kV]


% Ouput voltage converted to 3-phase and [kV]
solution.V_rms_3phs_kV = V_rms_3phs_kV;
solution.phase_shift_deg = phase_shift_deg;
solution.RL = RL;
solution.LL = LL;


% DC step response values
%[stepResponse.y, stepResponse.t] = step(sys, ts);
%stepResponse.uDC= V_1phs_rms;

end
```

```
Not enough input arguments.
Error in evaluateSSModel (line 27)
S_pu = S_input;                     % Apparent power delivered to load in
p.u. base.
```

Published with MATLAB® R2023b

Table of Contents


```
function [solution, graph] = evaluateSSModelDC(S_input, sampling)
%{
******************************************************
Purpose:
    Simulate a DC equivalent, expressed in state space,
    of a two bus system  and compare the output voltage
    and phase angle against a sinusoidal input.

Author:
    Kestutis Samulis, Mai 24, 2024
******************************************************
%}

f = 50;                                 % Frequency
w = 2*pi*f;                             % Angular frequency [rad/s]

% Specified base values
S_base = 1e6;                           % S_base [VA] is specified for a 3-phase
system.
V_base = 12500;                         % V_base [V] is the RMS voltage
specified for a 3-phase system.

% 3-phase RMS voltage
V_3phs_rms = V_base;                    % Base voltage is the RMS value of a
3-phase system
V_1phs_rms = V_3phs_rms/sqrt(3);        % Converting 3-phase rms voltage to
single-phase voltage

% Converting 3-phase apparent power to single-phase
%S_pu = 0.1 + j*0.1;                      % Apparent power delivered to load in
p.u. base.
S_pu = S_input;                         % Apparent power delivered to load in
p.u. base.
S_3phs_actual = S_pu*S_base;            % Converting p.u. value to actual value
for a 3-phase system.
S_1phs_actual = S_3phs_actual/3;        % Conveting the 3-phase apparent power
to single-phase apparent power.

% Finding load impedance
Z_load = (V_1phs_rms^2)/S_1phs_actual;

% Specified values for circuit components
C1 = 1e-7;                  % Capacitor in parallel with RS and RT
C2 = 1e-7;                  % Capacitor in parallel with LT and RL
Rs = 0.01;                  % Resistor in series with the voltage source
RT = 0.4688;                % Transmission line resistor
LT = 0.003;                 % Transmission line inductor
```

```
RL = real(Z_load);        % Load resistor
LL = -imag(Z_load)/w;     % Load inductor

% State space model of the two bus system
A = [ -1/(C1*Rs)     -1/C1        0        0;
       1/LT          -(RT/LT)    -1/LT     0;
       0             1/C2         0       -1/C2;
       0             0            1/LL     -(RL/LL)];
B = [1/(C1*Rs); 0;  0;  0];
C = [0 0 1 0];
D = 0;

% Sampling time
Fs = sampling.Fs;  % Sampling frequency
t0 = sampling.t0;  % Initial time
tf = sampling.tf;  % Final time
dt = 1/Fs;         % Time step
ts = t0:dt:tf;     % Sampling time


u = V_1phs_rms*ones(size(ts));          % Single-phase input voltage
oscillating sinusoidally

sys = ss(A, B, C, D);

% State initial condition
x0 = [0;0;0;0];

% Simulate system's output behaviour to the applied input voltage
[y, t] = lsim(sys, u, ts, x0);

% Sinusoidal input and ouput voltages with V_peak_1phs as magnitude
graph.t = t;
graph.u = u;
graph.y = y;

solution.V_phs_rms = V_1phs_rms;
solution.RL = RL;
solution.LL = LL;

end

Not enough input arguments.
Error in evaluateSSModelDC (line 27)
S_pu = S_input;                    % Apparent power delivered to load in
p.u. base.
```

Published with MATLAB® R2023b

Table of Contents


```
function [solution,graph] = fourbusSystem(S_input,sampling)
%{
******************************************************
Purpose:
    Simulate a DC equivalent, expressed in state space,
    of a two bus system  and compare the output voltage
    and phase angle against a sinusoidal input.

Author:
    Kestutis Samulis, Mai 24, 2024
******************************************************
%}

solution = struct();    % Array of solutions for each bus
graph = struct();       % Graph for each bus

    % S_input = 0.4+j*0.2               % Used when testing
    f = 50;                             % Frequency
    w = 2*pi*f;                         % Angular frequency [rad/s]

    % Specified base values
    S_base = 1e6;                       % S_base [VA] is specified for a 3-
phase system.
    V_base = 12500;                     % V_base [V] is the RMS voltage
specified for a 3-phase system.

    % 3-phase RMS voltage
    V_3phs_rms = V_base;                % Base voltage is the RMS value of a
3-phase system
    V_1phs_rms = V_3phs_rms/sqrt(3);    % Converting 3-phase rms voltage to
single-phase voltage
    % Voltage magnitude is converted to peak voltage for single-phase
    V_3phs_peak = V_3phs_rms * sqrt(2);   % Peak voltage of a 3-phase system
    V_1phs_peak = V_3phs_peak/sqrt(3);    % Converting peak voltage from 3-
phase to single-phase


    % Converting 3-phase apparent power to single-phase
    %S_pu = 0.1 + j*0.1;                  % Apparent power delivered to load
in p.u. base.
    S_pu = S_input;                     % Apparent power delivered to load
in p.u. base.
    S_3phs_actual = S_pu*S_base;        % Converting p.u. value to actual
value for a 3-phase system.
    S_1phs_actual = S_3phs_actual/3;    % Conveting the 3-phase apparent
power to single-phase apparent power.
```

```
    % Finding load impedance
    Z_load = (V_1phs_rms^2)/S_1phs_actual;

    % Specified values for circuit components
    Rs = 0.01;                % Resistor in series with the voltage source
    CT2 = 1e-7;                % Capacitor in parallel with RS and RT
    CT3 = 1e-7;                % Capacitor in parallel with LT and RL
    CT4 = 1e-7;
    CT6 = 1e-7;
    %CT6 = 1e-14;
    RT2 = 0.4688;
    LT2 = 0.003;
    RL2 = 1.547;
    LL2 = 0.049243;
    RT3 = 0.4688;
    LT3 = 0.003;
    RL3 = 1.547;
    LL3 = 0.049243;
    RT4 = 0.4688;
    LT4 = 0.003;
    RL4 = real(Z_load);
    LL4 = -imag(Z_load)/w;

    % State space model of a four bus system
    A = [-RT2/LT2 -1/LT2 0 1/LT2 0 0 0 0 0 0;
         1/CT2 0 -1/CT2 0 0 0 0 0 0 0;
         0 1/LL2 -RL2/LL2 0 0 0 0 0 0 0;
         -1/CT3 0 0 -1/(Rs*CT3) -1/CT3 0 0 0 0 0;
         0 0 0 1/LT3 -RT3/LT3 -1/LT3 0 0 0 0;
         0 0 0 0 1/CT4 0 -1/CT4 -1/CT4 0 0;
         0 0 0 0 0 1/LL3 -RL3/LL3 0 0 0;
         0 0 0 0 0 1/LT4 0 -RT4/LT4 -1/LT4 0;
         0 0 0 0 0 0 0 1/CT6 0 -1/CT6;
         0 0 0 0 0 0 0 0 1/LL4 -RL4/LL4;];

    B = [0; 0; 0; 1/(Rs*CT3); 0; 0; 0; 0; 0; 0;];

    D = 0;

%Output
% V2 = voltage at bus 2
% V3 = voltage at bus 1
% V4 = voltage at bus 3
% V6 = voltage at bus 4
    C = [0 1 0 0 0 0 0 0 0 0
         0 0 0 1 0 0 0 0 0 0
         0 0 0 0 0 1 0 0 0 0
         0 0 0 0 0 0 0 0 1 0];


    sys = ss(A, B, C, D);

    sampling.Fs = 1000000;     % Sampling frequency
    sampling.t0 = 0;           % Initial time
```

```
    sampling.tf = 0.1;        % Final time

    % Sampling time
    Fs = sampling.Fs;  % Sampling frequency
    t0 = sampling.t0;  % Initial time
    tf = sampling.tf;  % Final time
    dt = 1/Fs;         % Time step
    ts = t0:dt:tf;     % Sampling time


    % Initial condition
    x0 = [0;0;0;0;0;0;0;0;0;0];

    % Input voltage
    u = V_1phs_peak * sin(w*ts);   % Single-phase input voltage oscillating
sinusoidally

    % Simulate system's output behaviour to the applied input voltage
    [y, t] = lsim(sys, u, ts, x0);

    % Sinusoidal input and ouput voltages with V_peak_1phs as magnitude



    u = u';
    [pks_u_1phs, locs_u] = findpeaks(u(: ,1), t(:, 1));
    locs_end_u = locs_u(end);
    pks_end_u_1phs = pks_u_1phs(end); % u - 1 phase peak to peak


    [~, NumCol] = size(y);
    pks_y_1phs = cell(NumCol, 1);   % y - 1 phase peak to peak
    locs_y = cell(NumCol, 1);

    locs_end_y = cell(NumCol, 1);
    pks_end_y_1phs = cell(NumCol, 1); % y(end) - 1 phase peak to peak
    pks_end_y_3phs = cell(NumCol, 1); % y(end) - 3 phase peak to peak
    rms_y_3phs = cell(NumCol, 1); % y(end) - 3 phase rms

    time_diff = cell(NumCol, 1);
    phs_deg = cell(NumCol, 1);

    mag_diff_1phs = cell(NumCol, 1);
    mag_diff_percent_1phs = cell(NumCol, 1);

    mag_diff_3phs_peak = cell(NumCol, 1);
    mag_diff_3phs_rms = cell(NumCol, 1);

    for i=1:NumCol
      w = 360*f; % angular frequency in degrees

      % STEADY STATE
      [pks_y_1phs{i}, locs_y{i}] = findpeaks(y(:, i), t(:, 1));
```

```
        % PHASE ANGLE
        locs_end_y{i} = locs_y{i}(end);
        time_diff{i} = locs_end_u-locs_end_y{i};
        phs_deg{i} = (w*time_diff{i});                          % PHASE ANGLE
(OUTPUT)

        % 1 PHASE
        pks_end_y_1phs{i} = pks_y_1phs{i}(end);                  % 1-phase
MAGNITUDE (OUTPUT)
        mag_diff_1phs{i} = pks_end_u_1phs-pks_end_y_1phs{i};  % 1-phase
MAGNITUDE Diff (OUTPUT)
        mag_diff_percent_1phs{i} = 1-(pks_end_y_1phs{i}/pks_end_u_1phs);   %
y/u percent 1 phase

        % 3-PHASE (SCALING FROM 1 PHASE)
        pks_end_y_3phs{i} = pks_end_y_1phs{i}*sqrt(3);          % 1phase -->
3phase
        mag_diff_3phs_peak{i} = (pks_end_u_1phs*sqrt(3)) - pks_end_y_3phs{i};
% 3-phase MAGNITUDE DIFF

        rms_y_3phs{i} = pks_end_y_3phs{i}/sqrt(2);               % 3-phase RMS
MAGNITUDE (OUTPUT)
        mag_diff_3phs_rms{i} = mag_diff_3phs_peak{i}/sqrt(2);       % 3-phase
RMS MAGNITUDE DIFF (OUTPUT)
    end

    % RETURN
    solution.phs_deg = phs_deg;
    solution.rms_y_3phs = rms_y_3phs;
    solution.mag_diff_3phs_rms = mag_diff_3phs_rms;

    % 3 PHASE RMS
    graph.t = t;
    graph.u = u * sqrt(3)/sqrt(2); % 3 PHASE RMS INPUT
    graph.y = y * sqrt(3)/sqrt(2);  % 3 PHASE RMS OUTPUTS

end

Not enough input arguments.
Error in fourBusSystem (line 35)
    S_pu = S_input;                     % Apparent power delivered to load
in p.u. base.
```

Published with MATLAB® R2023b

Table of Contents


```
function [apparentPower] = inputGenerator(n, options)

rng(options.seed)

startVal = options.startVal;
endVal = options.endVal;

if options.keepReConst == true

real = options.const;
imag = startVal + (endVal-startVal) * rand(n,1);

elseif options.keepImConst == true

real = startVal + (endVal-startVal) * rand(n,1);
imag = options.const;

else

real = startVal + (endVal-startVal) * rand(n,1);
imag = startVal + (endVal-startVal) * rand(n,1);

end

apparentPower = sort(real) + i*sort(imag);
```

```
Not enough input arguments.
Error in inputGenerator (line 3)
rng(options.seed)
```

Published with MATLAB® R2023b

Table of Contents


```
clear all, clc; close all
%{
******************************************************
Purpose:
    Simulate a DC equivalent, expressed in state space,
    of a two bus system  and compare the output voltage
    and phase angle against a sinusoidal input.

Author:
    Kestutis Samulis, Mai 24, 2024
******************************************************
%}
programPara.showSolutionsInCmd = true;      % Show SS vs NR solutions graph
programPara.plotModelComparison = true;     % Show solutions in cmd window
```

Generate input data

```
%{
**************************************************************************
inputGenerator function generates random complex values from a uniform
distribution. The returned complex value array is sorted to be in increasing
order. Start and end values are spesified in a struct called 'options'.
n, specifies the total number of complex values to be generated.
**************************************************************************
%}

% Parameters
options.startVal = 0.1;
options.endVal = 2;
options.keepReConst = false;
options.keepImConst = false;
options.const = 0.2;
options.seed = 42;
n = 20;

% The function returns an array of randomized complex values in increasing
% order
SpowerArr = inputGenerator(n,options);
```

Simulate State Space model (2 bus system)

```
degree_symbol = char(176);
phase_symbol = char(8736);


% Sampling time
sampling.Fs = 1000000;     % Sampling frequency
sampling.t0 = 0;           % Initial time
sampling.tf = 0.2;         % Final time


% Solution array for State Space method
solArrSS = {};


if programPara.showSolutionsInCmd % Displays the title if true
disp('STATE-SPACE MODEL SOLUTIONS')
fprintf('itr. |VLL_3phs|%sangl%s [kV]\tApparent power values (input)\n' ...
        ,phase_symbol, degree_symbol);
disp('-------------------------------------------------------------------')
end

for i = 1:n

Spu = SpowerArr(i); % input array
[solSS] = evaluateSSModel(Spu, sampling); % Two bus system

% Plot values for output, input and time
%y = graph.y;     % output voltage
%u = graph.u;     % input voltage
%t = graph.t;     % time

% Output voltage magnitude and angle converted to 3-phase
Vrms3phskV = solSS.V_rms_3phs_kV;        % Voltage at bus #2
phaseShiftDeg = solSS.phase_shift_deg;   % Phase at bus #2

if programPara.showSolutionsInCmd % Displays the results if true
fprintf('%d.\t',i)
fprintf(' %.2f %s %.2f %s [kV] \t', ...
    Vrms3phskV, phase_symbol, phaseShiftDeg, degree_symbol)
fprintf('S = %s \t[pu]\n',num2str(Spu))
end

% Solution array
solArrSS{end+1} = [Vrms3phskV, phaseShiftDeg];

end
```

```
STATE-SPACE MODEL SOLUTIONS
itr. |VLL_3phs|∠angl° [kV]    Apparent power values (input)
-------------------------------------------------------------------
1.     12.48 ∠ -0.02 ° [kV]     S = 0.13911+0.18826i     [pu]
```

```
2.      12.48 ∠ -0.04 ° [kV]      S = 0.21036+0.2236i      [pu]
3.      12.46 ∠ -0.09 ° [kV]      S = 0.39639+0.28558i      [pu]
4.      12.46 ∠ -0.07 ° [kV]      S = 0.39644+0.36504i      [pu]
5.      12.45 ∠ -0.07 ° [kV]      S = 0.44547+0.424i      [pu]
6.      12.45 ∠ -0.07 ° [kV]      S = 0.44847+0.47938i      [pu]
7.      12.43 ∠ -0.05 ° [kV]      S = 0.50344+0.65507i      [pu]
8.      12.42 ∠ -0.11 ° [kV]      S = 0.65334+0.67877i      [pu]
9.      12.41 ∠ -0.09 ° [kV]      S = 0.67806+0.79609i      [pu]
10.      12.40 ∠ -0.11 ° [kV]      S = 0.81163+0.93629i      [pu]
11.      12.39 ∠ -0.14 ° [kV]      S = 0.9207+0.96653i      [pu]
12.      12.38 ∠ -0.20 ° [kV]      S = 1.097+1.077i      [pu]
13.      12.36 ∠ -0.22 ° [kV]      S = 1.2375+1.2256i      [pu]
14.      12.36 ∠ -0.22 ° [kV]      S = 1.2421+1.2543i      [pu]
15.      12.35 ∠ -0.27 ° [kV]      S = 1.4453+1.2625i      [pu]
16.      12.34 ∠ -0.27 ° [kV]      S = 1.4908+1.4i      [pu]
17.      12.32 ∠ -0.31 ° [kV]      S = 1.6816+1.5918i      [pu]
18.      12.31 ∠ -0.31 ° [kV]      S = 1.7457+1.636i      [pu]
19.      12.29 ∠ -0.32 ° [kV]      S = 1.9064+1.9029i      [pu]
20.      12.28 ∠ -0.32 ° [kV]      S = 1.9428+1.9347i      [pu]
```

Simulate Newton-Rhapson method (2 bus system)

```
degree_symbol = char(176);
phase_symbol = char(8736);

% Solution array for Newton-Rhapson method
solArrNR = {};

if programPara.showSolutionsInCmd
disp('NEWTON-RAPHSON METHOD SOLUTIONS')
fprintf('itr. |VLL_3phs|%sangl%s [kV]\tApparent power values (input)\n' ...
        ,phase_symbol, degree_symbol);
disp('-----------------------------------------------------------------')
end

for i = 1:n

Spu = SpowerArr(i);
[solNR] = evaluateNRMethod(Spu);

% Output voltage magnitude and angle converted to 3-phase
Vrms3phskV = solNR.v2;                  % Voltage at bus #2
phaseShiftDeg = solNR.d2;               % Phase at bus #2

if programPara.showSolutionsInCmd   % Displays the results if true
%disp('3-phase VLL output voltage and phase angle is')
fprintf('%d.\t',i)
fprintf(' %.2f %s %.2f %s [kV] \t', ...
    Vrms3phskV, phase_symbol, phaseShiftDeg, degree_symbol)
fprintf('S = %s \t[pu]\n',num2str(Spu))
end
```

```
% Solution array
solArrNR{end+1} = [Vrms3phskV, phaseShiftDeg];

end
```

```
NEWTON-RAPHSON METHOD SOLUTIONS
itr. |VLL_3phs|∠angl° [kV]    Apparent power values (input)
-----------------------------------------------------------------
1.      12.48 ∠ -0.02 ° [kV]      S = 0.13911+0.18826i      [pu]
2.      12.48 ∠ -0.03 ° [kV]      S = 0.21036+0.2236i      [pu]
3.      12.46 ∠ -0.09 ° [kV]      S = 0.39639+0.28558i      [pu]
4.      12.46 ∠ -0.07 ° [kV]      S = 0.39644+0.36504i      [pu]
5.      12.45 ∠ -0.08 ° [kV]      S = 0.44547+0.424i      [pu]
6.      12.45 ∠ -0.07 ° [kV]      S = 0.44847+0.47938i      [pu]
7.      12.43 ∠ -0.06 ° [kV]      S = 0.50344+0.65507i      [pu]
8.      12.42 ∠ -0.11 ° [kV]      S = 0.65334+0.67877i      [pu]
9.      12.41 ∠ -0.10 ° [kV]      S = 0.67806+0.79609i      [pu]
10.      12.40 ∠ -0.12 ° [kV]      S = 0.81163+0.93629i      [pu]
11.      12.39 ∠ -0.15 ° [kV]      S = 0.9207+0.96653i      [pu]
12.      12.38 ∠ -0.19 ° [kV]      S = 1.097+1.077i      [pu]
13.      12.36 ∠ -0.22 ° [kV]      S = 1.2375+1.2256i      [pu]
14.      12.36 ∠ -0.21 ° [kV]      S = 1.2421+1.2543i      [pu]
15.      12.35 ∠ -0.28 ° [kV]      S = 1.4453+1.2625i      [pu]
16.      12.34 ∠ -0.28 ° [kV]      S = 1.4908+1.4i      [pu]
17.      12.31 ∠ -0.31 ° [kV]      S = 1.6816+1.5918i      [pu]
18.      12.31 ∠ -0.32 ° [kV]      S = 1.7457+1.636i      [pu]
19.      12.28 ∠ -0.33 ° [kV]      S = 1.9064+1.9029i      [pu]
20.      12.28 ∠ -0.34 ° [kV]      S = 1.9428+1.9347i      [pu]
```

Plotting State-Space model comparison against Newton-Raphson method (2 bus system)

```
if programPara.plotModelComparison

    % Close all open figures if any exist
    figHandles = findobj('Type', 'figure');
    if ~isempty(figHandles)
        close(figHandles);
    end

    % Hold the values
    x = zeros(1, numel(solArrSS));
    y = zeros(1, numel(solArrSS));

    for i = 1:numel(solArrSS)
        % State Space
        xSS(i) = solArrSS{i}(1); % Voltage
        ySS(i) = solArrSS{i}(2); % Angle
```

```
        % Newton-Raphson
        xNR(i) = solArrNR{i}(1); % Voltage
        yNR(i) = solArrNR{i}(2); % Angle
    end

    f1 = figure;
    f1.Position = [2500 300 540 400];
    %set(f1, 'WindowState', 'maximized');
    set(gcf, 'Units', 'Normalized', 'OuterPosition', [0.2, 0.3, 0.4, 0.46]);
    plot(xSS, ySS, '-.*', 'LineWidth', 1.5, 'MarkerSize', 5,
'MarkerFaceColor', 'b');
    hold on
    plot(xNR, yNR, '-.^', 'LineWidth', 1.5, 'MarkerSize', 3,
'MarkerFaceColor', 'r');
    grid on;
    title('State-Space Model Solutions vs Newton-Raphson Method Solutions');
    xlabel('Voltage magnitude [kV]');
    ylabel('Phase angle [deg]');
    legend('State Space model', 'Newton-Raphson method');

end
```

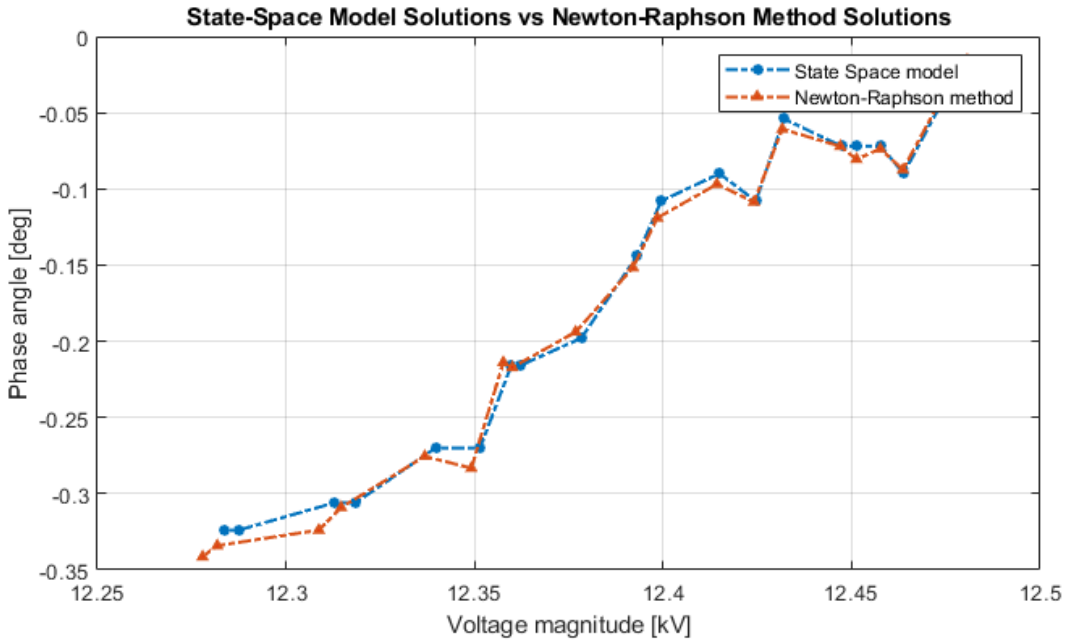

State space model DC vs AC response (2 bus system)

```
%INPUT
Spu = 10 + 10i;


% Sampling time
```

```
sampling.Fs = 1000000;     % Sampling frequency
sampling.t0 = 0;           % Initial time
sampling.tf = 0.1;         % Final time

% DC response
[solSSDC, graphDC] = evaluateSSModelDC(Spu, sampling);

% Plot values for output
yDC = graphDC.y;     % output voltage
uDC = graphDC.u;     % input voltage
tDC = graphDC.t;     % time

f2 = figure;
f2.Position = [2500 300 540 400];
subplot(2,1,1)
%set(f1, 'WindowState', 'maximized');
set(gcf, 'Units', 'Normalized', 'OuterPosition', [0.2, 0.3, 0.4, 0.46]);
plot(tDC, yDC,'LineWidth',0.9)%, '-.*', 'LineWidth', 1.5, 'MarkerSize', 5,
'MarkerFaceColor', 'b');
hold on
plot(tDC, uDC);
ytickformat('%.f');
ax1 = gca;
ax1.YAxis.Exponent = 0; % Disable scientific notation
legend('V_2', 'V_s{rms}');
text = 'Dynamic model response with DC input, $V_{rms}$';
font = title(text, 'Interpreter', 'latex', 'FontWeight','bold');
font.FontSize = 12;
xlabel('Time [s]');
ylabel('Voltage [V]');

% AC response
[solSSAC, graphAC] = evaluateSSModel(Spu, sampling);

% Plot values for output
yAC = graphAC.y;     % output voltage
uAC = graphAC.u;     % input voltage
tAC = graphAC.t;     % time

subplot(2,1,2)
%set(f1, 'WindowState', 'maximized');
set(gcf, 'Units', 'Normalized', 'OuterPosition', [0.2, 0.3, 0.4, 0.46]);
plot(tAC, yAC,'LineWidth',0.9)%, '-.*', 'LineWidth', 1.5, 'MarkerSize', 5,
'MarkerFaceColor', 'b');
hold on
plot(tAC, uAC);
ytickformat('%.f');
ax2 = gca;
ax2.YAxis.Exponent = 0; % Disable scientific notation
legend('V_2', 'V_s');
text = 'Dynamic model response with AC input, $V_{peak}\cdot\sin(\omega t)$';
font = title(text, 'Interpreter', 'latex', 'FontWeight','bold');
font.FontSize = 12;
xlabel('Time [s]');
```

```
ylabel('Voltage [V]');

fprintf('\nSTATE-SPACE MODEL DC vs AC INPUT RESPONSE\n')
fprintf('RL = %.3f [\x2126] \nLL = %.3f [H]\n\n', solSSAC.RL,solSSAC.LL)
```

```
STATE-SPACE MODEL DC vs AC INPUT RESPONSE
RL = 7.813 [Ω]
LL = 0.025 [H]
```

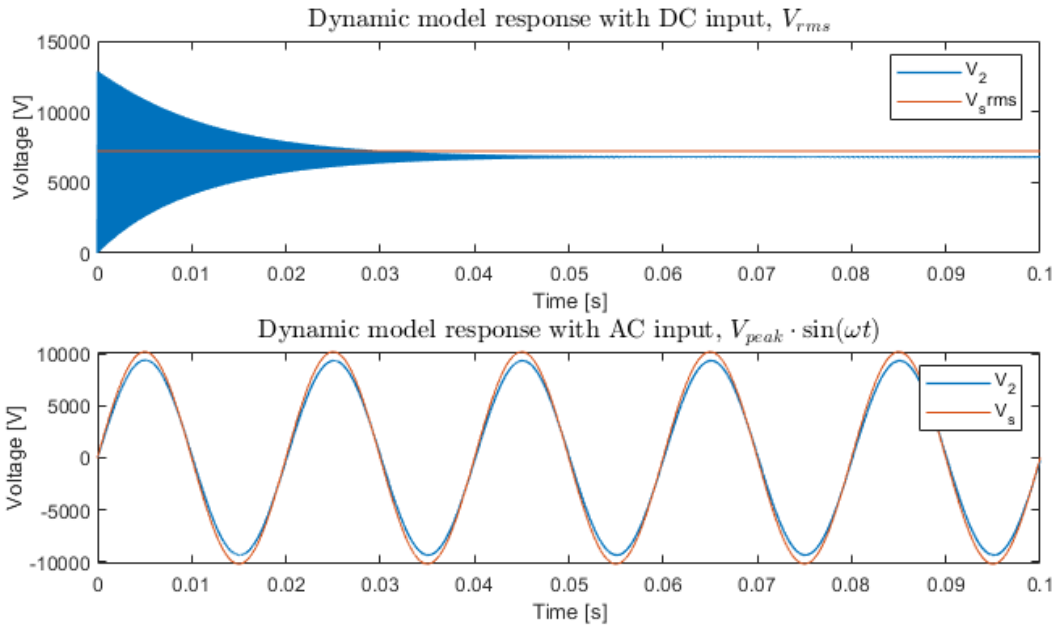

(4 bus system)

```
%INPUT
%Spu = 0.4 + j*0.2;
Spu = 0.8 + j*0.6;

% Sampling time
sampling.Fs = 1000000;     % Sampling frequency
sampling.t0 = 0;           % Initial time
sampling.tf = 0.1;         % Final time

% DC response
[solSS4, graph4] = fourBusSystem(Spu, sampling);


f2 = figure;
f2.Position = [2500 300 540 400];
%set(f1, 'WindowState', 'maximized');
set(gcf, 'Units', 'Normalized', 'OuterPosition', [0.2, 0.1, 0.4, 0.8]);
%[0.2, 0.3, 0.4, 0.46]);
```

```
%set(gcf, 'DefaultAxesLooseInset', [20, 0.05, 10, 0.05]); % Modify as needed

n=1;
subplot(4,1,n)
plot(graph4.t(:,1) , graph4.y(:,n),'LineWidth',0.9)%, '-.*', 'LineWidth',
1.5, 'MarkerSize', 5, 'MarkerFaceColor', 'b');
hold on
plot(graph4.t(:,1), graph4.u(:,1));
ytickformat('%.f');
ax1 = gca;
ax1.YAxis.Exponent = 0; % Disable scientific notation
legend('V_1', 'V_s');
xlabel('Time [s]');
ylabel('Voltage [V]');
text = 'Voltage at bus 1';
title(text);
%font.FontSize = 12;


n=2;
subplot(4,1,n)
plot(graph4.t(:,1) , graph4.y(:,n),'LineWidth',0.9)%, '-.*', 'LineWidth',
1.5, 'MarkerSize', 5, 'MarkerFaceColor', 'b');
hold on
plot(graph4.t(:,1), graph4.u(:,1));
ytickformat('%.f');
ax1 = gca;
ax1.YAxis.Exponent = 0; % Disable scientific notation
legend('V_2', 'V_s');
xlabel('Time [s]');
ylabel('Voltage [V]');
text = 'Voltage at bus 2';
title(text);


n = 3;
subplot(4,1,n)
plot(graph4.t(:,1) , graph4.y(:,n),'LineWidth',0.9)%, '-.*', 'LineWidth',
1.5, 'MarkerSize', 5, 'MarkerFaceColor', 'b');
hold on
plot(graph4.t(:,1), graph4.u(:,1));
ytickformat('%.f');
ax1 = gca;
ax1.YAxis.Exponent = 0; % Disable scientific notation
legend('V_3', 'V_s');
xlabel('Time [s]');
ylabel('Voltage [V]');
text = 'Voltage at bus 3';
title(text);


n=4;
subplot(4,1,n)
plot(graph4.t(:,1) , graph4.y(:,n),'LineWidth',0.9)%, '-.*', 'LineWidth',
```

```
1.5, 'MarkerSize', 5, 'MarkerFaceColor', 'b');
hold on
plot(graph4.t(:,1), graph4.u(:,1));
ytickformat('%.f');
ax1 = gca;
ax1.YAxis.Exponent = 0; % Disable scientific notation
legend('V_4', 'V_s');
xlabel('Time [s]');
ylabel('Voltage [V]');
text = 'Voltage at bus 4';
title(text);

solSS4.phs_deg
solSS4.rms_y_3phs
solSS4.mag_diff_3phs_rms

%fprintf('Bus\n')
%solSS4(1).V_rms_3phs_kV
%solSS4(2).V_rms_3phs_kV
%solSS4(3).V_rms_3phs_kV
%solSS4(4).V_rms_3phs_kV
```

```
ans =
  4×1 cell array
    {[1.368]}
    {[0.072]}
    {[1.224]}
    {[1.008]}
ans =
  4×1 cell array
    {[11741]}
    {[12497]}
    {[11676]}
    {[11606]}
ans =
  4×1 cell array
    {[759.39]}
    {[2.9724]}
    {[824.34]}
    {[893.99]}
```

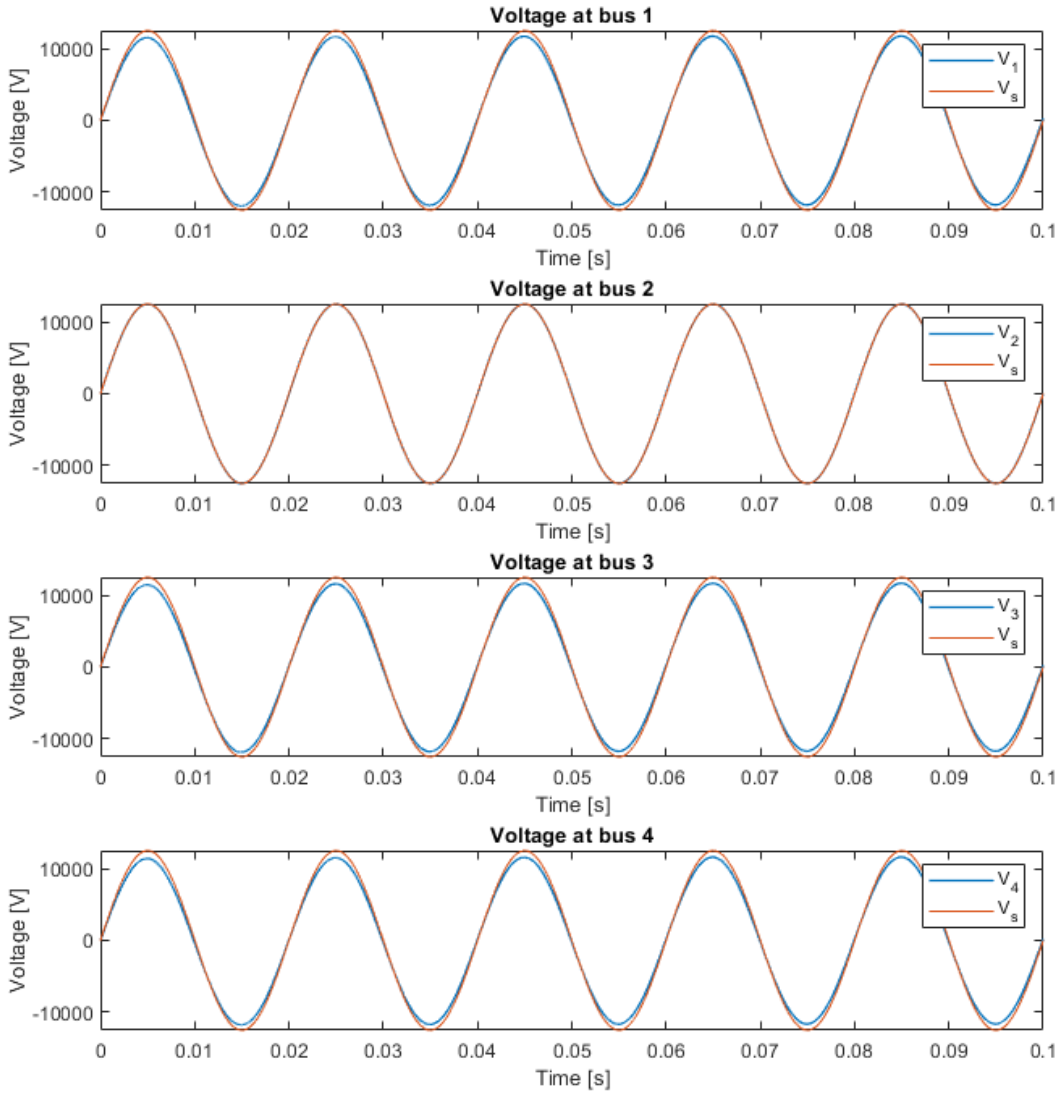

Log generated input data

```
%{
logFileName = 'workspace_log_A11.txt'
directory = 'C:\Users\kestu\OneDrive\Master\4. Semester\ELEMAS -
Sensitivity analysis for optimal operation of power distribution
networks\Programs\Matlab\Power flow model\MASTER\Log';
fullpath = fullfile(directory, logFileName);
logFile = fopen(fullpath, 'w');
for i = 1:length(SpowerArr)
    realPart = real(SpowerArr(i));
    imagPart = imag(SpowerArr(i));
```

```
    fprintf(logFile, '%.6f + i*%.6f\n', realPart, imagPart);
end
fclose(logFile);
%}
```

Published with MATLAB® R2023b